Figure 1 Generation of iPSCs from mouse AM and YS cells. (a) Isolation of AM and YS cells from the extra-embryonic tissues of newborn mice and generation of miPSCs through epigenetic reprogramming by retroviral infection–mediated expression of *Oct4*, *Sox2*, *Klf4* and *c-Myc*. (b) Expression of pluripotent cell marker proteins, alkaline phosphatase (ALP), Nanog, Oct4 and SSEA1. Cell nuclei were visualized with DAPI. (c) Transcriptional activation and silencing of pluripotent and somatic cell marker genes by miPSC induction. RT-PCR analyses revealed that pluripotent marker genes were activated, somatic marker genes were silenced, and *Klf4*, *c-Myc* and *Ronin* were expressed even in AM and YS cells. *Gapdh* is a positive control. Microarray analyses demonstrated global alteration in gene expression profile between YS cells and YS-miPSCs, which more closely resemble mESCs. Relative level of gene expression is illustrated as red > yellow > green. (d) The generation efficiency of ALP-positive colonies and timing of GFP detection demonstrating *Oct4-GFP* reporter gene reactivation. ALP-positive colonies (red) in a 10-cm culture dish was shown when 1.0×10^5 of AM cells, YS cells and MEFs were exposed to OSKM reprogramming factors and reseeded at day 4.

fully reprogrammed iPSCs (Sridharan & Plath 2008). Thus, the timing of reactivation of OG is closely linked with the efficiency of reprogramming. Activation of exogenous OG was detected in some cell populations in every colony around 10 days after OSKM transfection of AM and YS cells, similar to control MEFs examined here and those reported previously (Fig. 1d) (Brambrink *et al*. 2008). The reprogramming efficiency of AM and YS cells was estimated by ALP-staining 21 days after OSKM transfection with reseeding at day 4. Notably, the number of ALP-positive colonies was similar between AM cells (4373 ± 983; mean ± SEM, $n = 3$) and MEFs (4997 ± 1049, $n = 3$), and ~50% in YS cells (2293 ± 487, $n = 3$). Thus, the efficiency of AM reprogramming by OSKM is comparable to that of MEFs, and far exceeds that of adult somatic cells (Fig. 1d).

Germline-transmissible chimeras with AM and YS-miPSCs

To address *in vivo* differentiation potential of the AM and YS-miPSCs, approximately 10 agouti miPSCs were microinjected into C57BL/6J × BDF1 blastocysts (black), and transferred into white ICR foster mothers to generate chimeras. Three male YS-miPSC and two female AM-miPSC lines were tested for chimera formation. X-gal staining analysis on sections of E15.5 embryos demonstrated successful generation of normally developing chimeric embryos with OG/*Neo-LacZ* miPSC contribution to the majority of tissues in all miPSC lines examined (data not shown). We next examined the miPSC potential for normal growth to sexual maturity and germline transmission. Two high-degree chimeric mice with a YS-miPSC line and three high-degree chimeric mice with two AM-miPSC lines, characterized by the >50% contribution of agouti coat color (Fig. 2a), developed normally into adulthood. However, an adult YS-miPSC chimera developed a neck tumor around 8–10 weeks after birth, which may be due to reactivation of the exogenous *c-Myc* as reported previously (Nakagawa *et al.* 2008). Testes isolated from affected males were bisected and one-half was X-gal-stained for LacZ activity whereas the other half was cryosectioned. Blue staining in the seminiferous tubule indicated that YS-miPSCs could contribute to germ cell development. To confirm this, testis cryosections immunohistochemically stained with antibodies against LacZ (iPSC-derived cell marker) and TRA98 (spermatogonia and spermatocyte marker) (Fig. 2b). Germ cells in all tubules were positive for TRA98, whereas germ cells in only some seminiferous tubules were positive for LacZ, clearly demonstrating that YS-miPSCs are capable of contributing to the differentiating germ line in chimeras. Finally, to examine whether the genetic information of YS-miPSCs was transmissible to the next generation, DNA isolated from progeny of the remaining YS-miPSC chimera was analyzed by genomic PCR with a primer set specific to *Neo*. Seven of the thirty-five pups examined were positive, demonstrating that YS-miPSCs are able to differentiate into fully functional germ cells (Fig. 2c). In one of three female AM-miPSC chimeric mice, competence for contribution to germ cells was detected by X-gal staining analysis of ovaries (data not shown).

Teratoma formation with AM and YS-miPSCs

The differentiation competence of AM and YS-miPSCs was further tested by teratoma formation induced by injection of cells into the inguinal region of immunodeficient SCID mice. Teratomas were isolated 5–8 weeks after for histological analysis and for gene expression analysis. Hematoxylin–eosin (HE) staining of paraffin sections demonstrated that the three primary layers were generated as morphologically shown by ectodermal glia and neuroepithelium, mesodermal muscle and endodermal ciliated epithelium and cartilage (Fig. 2d). Multi-lineage differentiation of miPSCs was verified by transcription of endodermal, mesodermal and ectodermal genes in the majority of teratomas (Fig. 2e).

Generation of iPSCs from human AM cells

To examine whether hiPSCs could be efficiently generated from primary AM cells isolated from the amniotic membrane ($\sim$100 cm^2) of the placenta of newborn human (Fig. 3a), the reprogramming factors OCT4, SOX2, KLF4 and *c-MYC* were introduced by vesicular stomatitis virus G glycoprotein (VSV-G) retroviral transduction. About 20 AM-hiPSC lines were established from 1.0 × 10^5 AM cells infected (0.02%). The efficiency of AM-hiPSC generation is markedly high relative to that with cells from human adult tissues (Yu *et al.* 2007). AM-hiPSCs were morphologically similar to human ESCs (hESCs) (Fig. 3a). Immunohistochemical analyses demonstrated expression of the pluripotent cell-specific nuclear proteins OCT4, SOX2 and NANOG, and the keratan sulfate proteoglycan TRA-1-60 (Fig. 3b) consistent with the profile observed in hESCs. To extend this analysis, we examined the expression profile of genes by RT-PCR. The endogenous reprogramming factor genes OCT4, SOX2, KLF4 and *c-MYC* were all activated in AM-hiPSCs, whereas the transgenes were fully silenced (Fig. 3c). Expression of pluripotent cell-specific genes NANOG, REX1, GDF3, ESG1, FGF4, TERT and RONIN were also activated in all AM-hiPSC clones consistent with the profile of control hESCs (Fig. 3c). Notably, transcription of KLF4, *c-MYC*, and RONIN was detected not only in AM-hiPSCs but also AM cells. Similar to mouse AM and YS cells, endogenous expression of KLF4, *c-MYC* and RONIN in human AM cells may facilitate acquisition of reprogramming competency for efficient generation of hiPSCs.

DNA methylation of OCT4 and NANOG in AM-hiPSCs

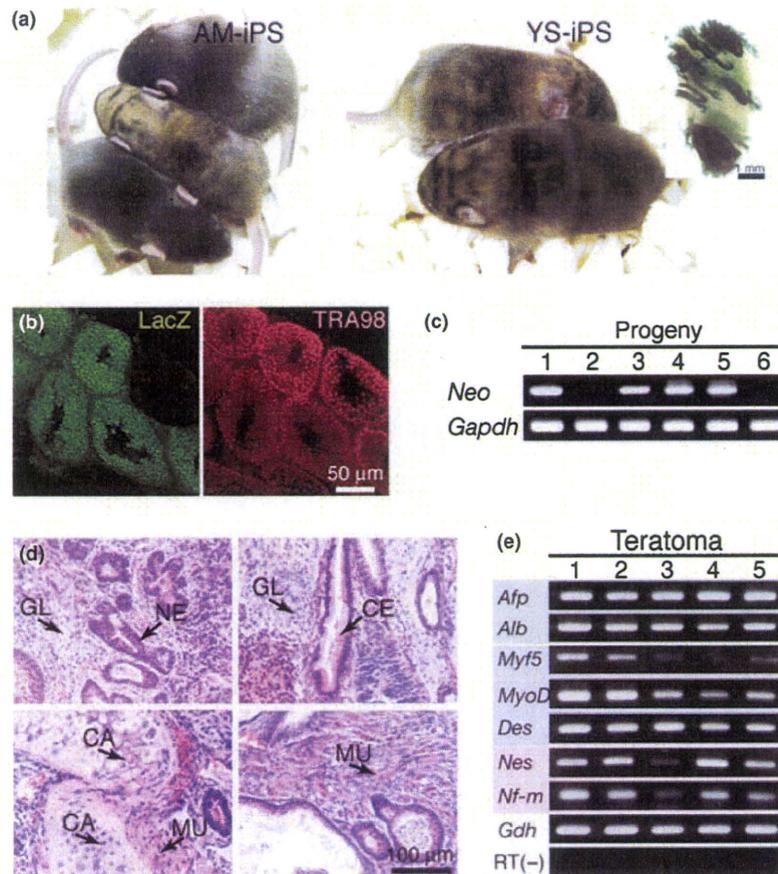To further characterize the pluripotent nature of AM-hiPSCs, the promoter CpG methylation status

Figure 2 Pluripotency of AM and YS–miPSCs. (a) Chimeric mice with female AM–miPSCs and male YS–miPSCs. Inset: X-gal staining of testis collected from an adult YS–miPSC chimera (blue cells are YS–miPSC derivatives). (b) Immunohistochemical double staining of testis cryosections from a YS–miPSC chimera with anti-LacZ (YS–miPSC-derived germ cells) and anti-TRA98 (spermatogonia and spermatocytes) antibodies. (c) Genotyping of progeny obtained by backcrossing with YS–miPSC chimeras. *Neo* positive demonstrates germline transmission of YS–miPSC genetic information. *Gapdh* is positive control. (d) Hematoxylin-eosin staining of teratoma sections generated by AM and YS–miPSC implantation. GL, glia (ectoderm); NE, neuroepithelium (ectoderm); CE, ciliated epithelium (endoderm); CA, cartilage (ectoderm); MU, muscle (mesoderm). (e) Transcription analysis of lineage-specific genes in teratomas generated with AM and YS–miPSCs. Gray rectangle: endoderm makers; purple rectangle: mesoderm markers; pink rectangle: ectoderm markers. *Afp*, α-*Fetoprotein*; *Alb*, *albumin*; *Des*, *desmin*; *Nes*, *Nestin*; *Nf-m*, *neurofilament-M*; *Gdh*, *Gapdh* (positive control).

of key pluripotency genes was examined by bisulfite-modified DNA sequencing. Promoters of both *OCT4* and *NANOG* were found to highly methylated in hAM cells, consistent with transcriptional silencing in these cells. Conversely, both promoter regions were hypo-methylated in AM-hiPSCs consistent with the observed reactivation (Fig. 3d). These data demonstrate that human AM cells are capable of being epigenetically reprogrammed to AM-hiPSCs through forced expression of reprogramming factors.

Teratoma formation with AM-hiPSCs

To address whether the AM-hiPSCs have competence to differentiate into specific tissues, teratoma formation was induced by implantation under the kidney capsule of immunodeficient nude mice. Twenty-one out of twenty-four AM-hiPS independent clones induced teratoma formation within 6–10 weeks of implantation (1.0×10^7 cells/site). Histological analysis by HE staining of paraffin-embedded sections demonstrated that the three
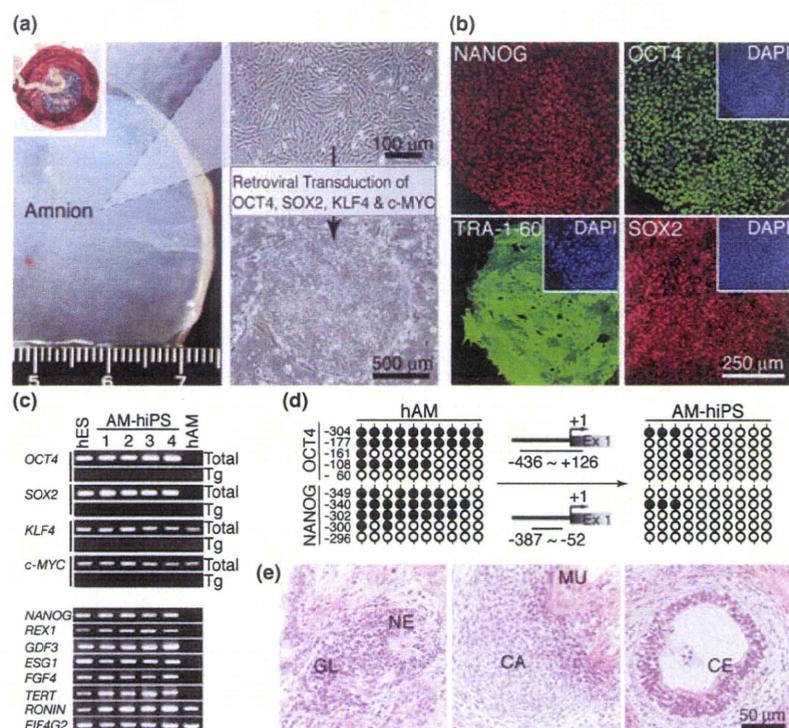
Figure 3 Generation of iPSCs from human AM cells. (a) Isolation of hAM cells from extra-embryonic tissues of human newborns and generation of hiPSCs through epigenetic reprogramming by retroviral infection-mediated expression of *OCT4*, *SOX2*, *KLF4* and *c-MYC*. (b) Expression of pluripotent cell marker proteins, NANOG, OCT4, TRA-1-60 and SOX2. Cell nuclei were visualized with DAPI. (c) Transcriptional activation of pluripotent marker genes by hiPSC induction. RT-PCR analyses revealed that the exogenous *OCT4*, *SOX2*, *KLF4* and *c-MYC* genes were silenced and the endogenous pluripotent marker genes were activated in AM-hiPSCs. *KLF4*, *c-MYC* and *RONIN* were expressed even in hAM cells before reprogramming. *EIF4G2* (*eukaryotic translation initiation factor 4 gamma 2*) is included as a positive control. (d) Epigenetic reprogramming of the *OCT4* and *NANOG* promoter regions. Bisulfite-modified DNA sequence analysis demonstrated a transition from hyper-methylation in AM cells (black circles) to hypo-methylation in AM-hiPSCs (white circles). (e) Hematoxylin-eosin staining of teratoma sections of teratoma generated by AM-hiPSC implantation. GL, glia (ectoderm); NE, neuroepithelium (ectoderm); CE, ciliated epithelium (endoderm); CA, cartilage (ectoderm); MU, muscle (mesoderm).

primary layers were generated as shown by ectodermal glia and neuroepithelium, mesodermal muscle and endodermal ciliated epithelium and cartilage morphologically (Fig. 3e). Thus, the majority of AM-hiPSC clones have potential for multi-lineage differentiation *in vivo*.

Discussion

We here demonstrated that hiPSCs and miPSCs were efficiently generated from newborn AM cells, in which endogenous *Klf4*, *c-Myc* and *Ronin* were highly expressed. The generation efficiency of miPSCs from AM cells was comparable to that from MEFs in mice and was notably high to that from adult somatic cells in humans. The properties of AM-hiPSCs and AM or YS-miPSCs resemble those of fully reprogrammed iPSCs from other tissues and ESCs.

iPSCs are generated through epigenetic reprogramming of somatic cells. Information on the base sequence of DNA in nuclei is unchanged through the reprogramming, although the gene expression profile is altered through the reprogramming from the somatic cell to the iPSC type. Developmentally rewound iPSCs retain aged DNA base sequence information inherited from somatic cells. The base sequence of DNA accumulates mutations through aging with cell division and mis-repair. Young somatic cells are suitable for iPSC generation rather than aged somatic cells. Therefore, it is suggested that the AM cells accumulating less genetic mutation are safer than the adult somatic cells as a cell source for iPSC generation.

The generation efficiency of OG-positive colonies was approximately four times lower than that of ALP-positive colonies and it is likely that miPSC generation will be further reduced (Wernig et al. 2008). Furthermore, when pre-iPSCs are reseeded, the generation efficiency of iPSC outcome could be roughly estimated as $1/2^X$ (X = reseeded day after infection or transfection; doubling time of pre-iPSC is estimated as 24 h). Recently, iPSC generation technology has been developed and improved with MEFs and human embryonic or newborn fibroblasts (HNFs) as representative somatic cells. Even with these types of cells, application of the current technology resulted in a marked decrease in iPSC generation efficiency. The retroviral transduction-mediated miPSC generation efficiency is 0.05–0.1% with MEFs (Takahashi et al. 2007; Wernig et al. 2007). The generation efficiency of hiPSCs (~0.01% in ALP-positive colony and 0.0025% in hiPSC outcome) (Yu et al. 2007; Wernig et al. 2008) is ~10 times lower than that of miPSCs. The generation efficiency of genetic modification-free hiPSCs from HNFs by direct delivery of reprogramming proteins is estimated at about 0.001% in outcome (Kim et al. 2009). Notably, it is evident that the generation of hiPSCs from adult somatic cells is much harder than that from MEFs. In fact, analysis with a secondary dox-inducible transgene system shows that the efficiency varies between different somatic cell types (Wernig et al. 2008). Thus, for practical application of iPSC technology to medical care, identification of reprogramming-sensitive cell types is a key issue. Human primary keratinocytes are one candidate cell type for efficient generation of hiPSCs from adult patients (the efficiency of ALP-positive colony = 1.0%) (Aasen et al. 2008). Here, we have shown that human and mouse AM cells, in which the endogenous KLF4/Klf4, c-MYC/c-Myc and RONIN/Ronin are naturally expressed, are highly reprogramming-sensitive (hiPSC generation efficiency was approximately 0.02% in outcome). An important point is that relatively huge amounts of human AM cells can be collected from discarded AM membranes at birth with no risk to the individual. Furthermore, these cells can be kept in long-term storage without requirement for amplification by in vitro cell culture.

Our findings illustrate that human AM cells are a strong candidate cell source for collection and banking that could be retrieved on demand and used for generating personalized genetic modification-free iPSCs applicable for clinical treatment and drug screening.

Experimental procedures

Amnion and yolk sac cells

In mice, AM and YS membranes collected from E18.5 embryos from GOF-18/delta PE/GFP (Oct4-GFP) transgenic females (Yoshimizu et al. 1999) mated with 129/Rosa26 transgenic males (Friedrich & Soriano 1991) were digested with 0.1% collagenase (Wako, Osaka, Japan) and 20% fetal bovine serum (FBS) at 37 °C for 1 h, and then repeatedly passed through a 26-gauge needle. The cell suspension was cultured with mES medium (DMEM/F12 (Dulbecco's modified Eagle's medium/Ham's F12) (Wako) supplemented with 15% FBS, 10^{-4} M 2-mercaptoethanol (Sigma) and 1000 U/mL of recombinant leukemia inhibitory factor (Chemicon, Temecula, CA, USA) containing 5 ng/mL basic fibroblast growth factor (bFGF) (Peprotech, Rocky Hill, NJ, USA). Following culture for 2–3 days, the adherent AM and YS cells growing to near-confluence were applied for iPSC experiments.

In humans, the AM membrane was cut into tiny pieces with dissection scissors. The AM membrane pieces were cultured in DMEM with 10% FBS for 7–10 days. The adherent AM cells growing to near-confluence were applied for iPSC experiments. Primary AM cells were provided from the cell bank of RIKEN Bioresource Center, Japan.

Generation of iPSCs

In mouse, each of pMXs-Oct4, Sox2, Klf4, c-Myc and DsRed (an indicator of retroviral silencing) was transfected into the Plat-E cells using the FuGENE6 Transfection Reagent (Roche Diagnostics, Indianapolis, IN, USA). A 1 : 1 : 1 : 1 : 4 mixture of Oct4, Sox2, Klf4, c-Myc and DsRed retroviruses in supernatants with 4 μg/mL polybrene (Nacalai Tesque, Kyoto, Japan) was added to AM and YS cells at 1.0×10^5 cells per 3 cm well. At day 4 after infection, the cells were reseeded into a 10 cm culture dish on feeder cells with mES medium. Colonies were picked around day 20.

In humans, pMXs-OCT4, SOX2, KLF4 or c-MYC, pCL-GagPol, and pHCMV-VSV-G vectors were transfected into 293FT cells (Invitrogen, Carlsbad, CA, USA) using the TransIT-293 reagent (Mirus). A 1 : 1 : 1 : 1 mixture of OCT4, SOX2, KLF4 and c-MYC viruses in supernatant with 4 μg/mL polybrene were added to AM cells at 1.0×10^5 cells per 3 cm well. The cells were subcultured on feeder cells into a 10 cm dish with the iPSellon medium (Cardio) supplemented with 10 ng/mL bFGF (Wako) (hES medium). Colonies were picked up around day 28.

Immunocytochemistry

Human and mouse cells were fixed with 4% paraformaldehyde in phosphate-buffered saline (PBS) for 10 min at 4 °C. After washing with 0.1% Triton X-100 in PBS (PBST), the cells were prehybridized with blocking buffer for 1–12 h at 4 °C and then incubated with primary antibodies; anti-SSEA4

Table 1 Primers for RT-PCR and PCR

Gene name	5'-Forward-3'	5'-Reverse-3'
Mice		
Oct4 (total)	CTGAGGGCCAGGCAGGAGCACGAG	CTGTAGGGAGGGCTTCGGGCACTT
Oct4 (endogenous)	TCTTTCCACCAGGCCCCCGGCTC	TGCGGGCGGACATGGGGAGATCC
Oct4 (transgene)	CCCATGGTGGTGGTACGGGAATTC	AGTTGCTTTCCACTCGTGCT
Sox2 (total)	GGTTACCTCTTCCTCCCACTCCAG	TCACATGTGCGACAGGGGCAG
Sox2 (transgene)	CCCATGGTGGTGGTACGGGAATTC	TCTCGGTCTCGGACAAAAGT
Klf4 (total)	CACCATGGACCCGGGCGTGGCTGCCAGAAA	TTAGGCTGTTCTTTTCCGGGGCCACGA
Klf4 (endogenous)	GCGAACTCACACAGGCGAGAAACC	TCGCTTCCTCTTCCTCCGACACA
Klf4 (transgene)	CCCATGGTGGTGGTACGGGAATTC	GTCGTTGAACTCCTCGGTCT
c-Myc (total)	CAGAGGAGGAACGAGCTGAAGCGC	TTATGCACCAGAGTTTCGAAGCTGTTCG
c-Myc (endogenous)	CAGAGGAGGAACGAGCTGAAGCGC	AAGTTTGAGGCAGTTAAAATTATGGCTGAAGC
c-Myc (transgene)	CTCCTGGCAAAAGGTCAGAG	GACATGGCCTGCCCGGTTATTATT
Nanog	ATGAAGTGCAAGCGGTGGCAGAAA	CCTGGTGGAGTCACAGAGTAGTTC
Eras	CAAAGATGCTGGCAGGCAGCTACC	GACAAGCAGGGCAAAGGCTTCCTC
Gdf3	AGTTTCTGGGATTAGAGAAAGC	GGGCCATGGTCAACTTTGCCT
Rex1	GACATCATGAATGAACAAAAATG	CCTTCAGCATTTCTTCCCTG
Zfp296	AAGCACCCAGATCTGTTGACCT	GAGCCTCTGGGGTATCTAGG
Ronin	GCCTCAGAGCTAGAGGCTGCTACG	TGGAAGGAGTCACGAATTCTGCAG
Igf1	GGACCAGAGACCCTTTGCGGGG	GGCTGCTTTTGTAGGCTTCAGTGG
Cd6	CCTAAGCACCCTGAAGCAAG	ACAACTGGGAACCCACAAAGC
Gapdh	CCCACTAACATCAAATGGGG	CCTTCCACAATGCCAAAGTT
α-Fetoprotein	TCGTATTCCAACAGGAGG	CACTCTTCCTTCTGGAGATG
Albumin	AAGGAGTGCTGCCATGGTGA	CCTAGGTTTCTTGCAGCCTC
Myf-5	TGCCATCCGCTACATTGAGAG	CCGGGTAGCAGGCTGTGAGTTG
MyoD	GCCCGCGCTCCAACTGCTCTGAT	CCTACGGTGGTGCGCCCTCTGC
Desmin	TTGGGGTCGCTGCGGTCTAGCC	GGTCGTCTATCAGGTTGTCACG
Nestin	GGAGTGTCGCTTAGAGGTGC	TCCAGAAAGCCAAGAGAAGC
Neurofilament-M	GCCGAGCAGACCAAGGAGGCCATT	CTGGATGGTGTCCTGGTAGCTGCT
Neo	CGGCAGGAGCAAGGTGAGAT	CAAGATGGATTGCACGCAGG
Humans		
OCT4 (total)	GCCGTATGAGTTCTGTGG	TCTCCTTCTCCAGCTTCAC
SOX2 (total)	TAAGTACTGGCGAACCATCT	AAATTACCAACGGTGTCAAC
KLF4 (total)	ACTCGCCTTGCTGATTGTCT	GAACGTGGAGAAAGATGGGA
c-MYC (total)	GCGTCCTGGGAAGGGAGATCCGGAGC	TTGAGGGGCATCGTCGCGGGAGGCTG
NANOG	ATTATGCAGGCAACTCACTT	GATTCTTTACAGTCGGATGC
REX1	CAGATCCTAAACAGCTCGCAGAAT	GCGTACGCAAATTAAAGTCCAGA
GDF3	CTTATGCTACGTAAAGGAGCGGG	GTGCCAACCCAGGTCCCGGAAGTT
ESG1	ATATCCCGCCGTGGGTGAAAGTTC	ACTCAGCCATGGACTGGAGCATCC
FGF4	CTACAACGCCTACGAGTCCTACA	GTTGCACCAGAAAAGTCAGAGTTG
TERT	CCTGCTCAAGCTGACTCGACACCGTG	GGAAAAGCTGGCCCTGGGGTGGAGC
RONIN	CACTGTAGACAGCAGTCAGG	TGCCTTTCATCTCTTTCATC
EIF4G2	AAGGAAAGGGACTGAGTTTC	CCAAGAAAGCTTCTTCTTCA
Bis-OCT4	GATTAGTTTGGGTAATATAGTAAGGT	ATCCCACCCACTAACCTTAACCTCTA
Bis-NANOG	TGGTTAGGTTGGTTTTAAATTTTTG	AACCCACCCTTATAAATTCTCAATTA

(1 : 300) (Chemicon), anti-TRA-1–60 (1 : 300) (Chemicon), anti-Oct4 (1 : 50) (Santa Cruz Biotechnology, Santa Cruz, CA, USA), anti-Nanog (1 : 300) (ReproCELL, Tokyo, Japan), anti-Sox2 (1 : 300) (Abcam, Cambridge, UK) and/or anti-SSEA1 (1 : 1000) (DSHB) antibodies for 6–12 h at 4 °C. They were incubated with secondary antibodies; anti-rabbit IgG, anti-mouse IgG or anti-mouse IgM conjugated with Alexa 488 or 546 (1 : 500) (Molecular Probes, Eugene, OR, USA) in blocking buffer for 1 h at room temperature. The cells were counterstained with 4,6-diamidino-2-phenylindole (DAPI) and then mounted with a SlowFade light antifade kit (Molecular Probes). To examine germline competence,

cryosections of a half of a testis of 4- to 5-week-old chimeric mice were fixed with 4% paraformaldehyde in PBS for overnight at 4 °C, and then prehybridized with blocking buffer. The sections were double-stained with primary antibodies; anti-LacZ antibody (1 : 500) (Promega, Madison, WI, USA) specific to miPSC-derived cells and with anti-TRA98 antibody (1 : 500) specific to spermatogonia and spermatocytes. The remaining testis and ovaries were stained with X-gal.

RT-PCR

Total RNAs were isolated from mouse and human cells using the TRIzol (Invitrogen) and the RNeasy Plus Mini Kit (Qiagen, Valencia, CA, USA), respectively. cDNAs were synthesized from 1 μg total RNAs using Superscript III reverse transcriptase (Invitrogen) with random hexamers according to the manufacturer's instructions. Template cDNA was PCR-amplified with gene-specific primer sets (Table 1).

Gene expression microarray

Total RNA was extracted from mouse cells using the TRIzol Reagent. Double-stranded cDNA synthesized from the total RNA was amplified and labeled using the One-Cycle Target Labeling and Control Regents (Affymetrix, Santa Clara, CA, USA). Global gene expression was examined with the Gene-Chip Mouse Genome 430 2.0 Array (Affymetrix). The fluorescence intensity of each probe was quantified by using the GeneChip Analysis Suite 5.0 computer program (Affymetrix). The level of gene expression was determined as the average difference (AD). Specific AD levels were then calculated as percentages of the mean AD level of probe sets for housekeeping genes *Actin* and *Gapdh*. To eliminate changes within the range of background noise and to select the most differentially expressed genes, data were used only if the raw data values were less than 50 AD. Further data were analyzed with Gene-Spring GX 7.3.1 (Agilent Technologies, Santa Clara, CA, USA).

Reprogramming efficiency

The reprogramming efficiency of mouse YS and AM cells was estimated by counting the number of ALP-positive colonies 21 days after retroviral infection. The cells in 10 cm culture dish were fixed with 4% paraformaldehyde in PBS for 15 min at room temperature and washed with PBS. After treating with ALP stain (pH 9.0) for 30 min at room temperature, the number of ALP-positive cells was counted.

Chimera

AM-miPSCs (2n = 40, XX) and YS-miPSCs (2n = 40, XY) were microinjected into blastocysts (C57BL/6J × BDF1). The blastocysts were transferred into the uterus of pseudopregnant ICR female mice. Chimeric mice were mated with C57BL/6J

for examining germline transmission. The genotype of the progeny was determined with tail tip DNA by genomic PCR with a *Neo*-specific primer set (Table 1). All animal experiments were performed according to the guidelines of animal experiments of Kyoto University, Japan.

Teratoma

In mice, cell suspension of 1.0×10^6 AM or YS-miPSCs/100 μL DMEM/F12 was subcutaneously injected into the inguinal region of immunodeficient SCID mice (CLEA). In humans, the 1 : 1 mixture of the AM-hiPSC suspension and Basement Membrane Matrix (BD Biosciences, San Jose, CA, USA) were implanted at 1.0×10^7 cells/site under the kidney capsule of immunodeficient nude mice (CLEA). Teratomas surgically dissected out 5–8 weeks in mice and 6–10 weeks in human after implantation, were fixed with 4% paraformaldehyde in PBS, and embedded in paraffin. Sections at 10 μm in thickness were stained with HE.

Bisulfite-modified DNA sequencing

Genomic DNAs (1 μg) extracted from AM-hiPSCs and hAM cells were bisulfite-treated with EZ DNA methylation-Gold Kit (ZYMO Research, Orange, CA, USA) according to the manufacturer's instruction. The promoter regions of the human *NANOG* and *OCT4* genes were PCR-amplified with specific primer sets (Table 1). Ten clones of each PCR product were gel-purified, sub-cloned and sequenced with the SP6 universal primer.

Acknowledgements

References

Aasen, T., Raya, A., Barrero, M.J., Garreta, E., Consiglio, A., Gonzalez, F., Vassena, R., Bilic, J., Pekarik, V., Tiscornia, G., Edel, M., Boue, S. & Belmonte, J.C. (2008). Efficient and rapid generation of induced pluripotent stem cells from human keratinocytes. *Nat. Biotechnol.* **26**, 1276–1284.

Brambrink, T., Foreman, R., Welstead, G.G., Lengner, C.J., Wernig, M., Suh, H. & Jaenisch, R. (2008). Sequential expression of pluripotency markers during direct reprogramming of mouse somatic cells. *Cell Stem Cell* **2**, 151–159.

Curran, T., Miller, A.D., Zokas, L. & Verma, I.M. (1984). Viral and cellular fos proteins: a comparative analysis. *Cell* **36**, 259–268.

Feng, B., Ng, J.H., Heng, J.C. & Ng, H.H. (2009). Molecules that promote or enhance reprogramming of somatic cells to induced pluripotent stem cells. *Cell Stem Cell* **4**, 301–312.

Friedrich, G. & Soriano, P. (1991). Promoter traps in embryonic stem cells: a genetic screen to identify and mutate developmental genes in mice. *Genes Dev.* **5**, 1513–1523.

Jaenisch, R. & Young, R. (2008). Stem cells, the molecular circuitry of pluripotency and nuclear reprogramming. *Cell* **132**, 567–582.

Kim, D., Kim, C.H., Moon, J.I., Chung, Y.G., Chang, M.Y., Han, B.S., Ko, S., Yang, E., Cha, K.Y., Lanza, R. & Kim, K.S. (2009). Generation of human induced pluripotent stem cells by direct delivery of reprogramming proteins. *Cell Stem Cell* **4**, 472–476.

Nakagawa, M., Koyanagi, M., Tanabe, K., Takahashi, K., Ichisaka, T., Aoi, T., Okita, K., Mochiduki, Y., Takizawa, N. & Yamanaka, S. (2008). Generation of induced pluripotent stem cells without Myc from mouse and human fibroblasts. *Nat. Biotechnol.* **26**, 101–106.

Sridharan, R. & Plath, K. (2008). Illuminating the black box of reprogramming. *Cell Stem Cell* **2**, 295–297.

Takahashi, K., Okita, K., Nakagawa, M. & Yamanaka, S. (2007). Induction of pluripotent stem cells from fibroblast cultures. *Nat. Protoc.* **2**, 3081–3089.

Wernig, M., Lengner, C.J., Hanna, J., Lodato, M.A., Steine, E., Foreman, R., Staerk, J., Markoulaki, S. & Jaenisch, R. (2008). A drug-inducible transgenic system for direct reprogramming of multiple somatic cell types. *Nat. Biotechnol.* **26**, 916–924.

Wernig, M., Meissner, A., Foreman, R., Brambrink, T., Ku, M., Hochedlinger, K., Bernstein, B.E. & Jaenisch, R. (2007). In vitro reprogramming of fibroblasts into a pluripotent ES-cell-like state. *Nature* **448**, 318–324.

Yamanaka, S. (2007). Strategies and new developments in the generation of patient-specific pluripotent stem cells. *Cell Stem Cell* **1**, 39–49.

Yoshimizu, T., Sugiyama, N., De Felice, M., Yeom, Y.I., Ohbo, K., Masuko, K., Obinata, M., Abe, K., Scholer, H.R. & Matsui, Y. (1999). Germline-specific expression of the Oct-4/green fluorescent protein (GFP) transgene in mice. *Dev. Growth Differ.* **41**, 675–684.

Yu, J., Vodyanik, M.A., Smuga-Otto, K., Antosiewicz-Bourget, J., Frane, J.L., Tian, S., Nie, J., Jonsdottir, G.A., Ruotti, V., Stewart, R., Slukvin, I.I. & Thomson, J.A. (2007). Induced pluripotent stem cell lines derived from human somatic cells. *Science* **318**, 1917–1920.

Zhou, H., Wu, S., Joo, J.Y., Zhu, S., Han, D.W., Lin, T., Trauger, S., Bien, G., Yao, S., Zhu, Y., Siuzdak, G., Scholer, H.R., Duan, L. & Ding, S. (2009). Generation of induced pluripotent stem cells using recombinant proteins. *Cell Stem Cell* **4**, 381–384.

Cell
PRESS

A Small-Molecule Inhibitor of Tgf-β Signaling Replaces *Sox2* in Reprogramming by Inducing *Nanog*

Justin K. Ichida,[1,3,6] Joel Blanchard,[1,6] Kelvin Lam,[1,6] Esther Y. Son,[1,2,3,5,6] Julia E. Chung,[1,2,3] Dieter Egli,[1,3]
Kyle M. Loh,[1] Ava C. Carter,[1,3] Francesco P. Di Giorgio,[1,3] Kathryn Koszka,[1,3] Danwei Huangfu,[1] Hidenori Akutsu,[4]
David R. Liu,[5] Lee L. Rubin,[1,*] and Kevin Eggan[1,2,3,*]
[1]Harvard Stem Cell Institute, Department of Stem Cell and Regenerative Biology, Harvard University, Cambridge, MA 02138, USA
[2]Department of Molecular and Cellular Biology, Harvard University, Cambridge, MA 02138, USA
[3]Stowers Medical Institute, 1000 East 50th Street. Kansas City, MO 64110, USA
[4]Department of Reproductive Biology, National Research Institute for Child Health and Development, 2-10-1 Okura, Setagaya,
Tokyo 157-8535
[5]Howard Hughes Medical Institute and the Department of Chemistry and Chemical Biology, Harvard University, Cambridge, MA 02138, USA
[6]These authors contributed equally to this work
*Correspondence: lee_rubin@harvard.edu (L.L.R.), eggan@mcb.harvard.edu (K.E.)
DOI 10.1016/j.stem.2009.09.012

SUMMARY

The combined activity of three transcription factors can reprogram adult cells into induced pluripotent stem cells (iPSCs). However, the transgenic methods used for delivering reprogramming factors have raised concerns regarding the future utility of the resulting stem cells. These uncertainties could be overcome if each transgenic factor were replaced with a small molecule that either directly activated its expression from the somatic genome or in some way compensated for its activity. To this end, we have used high-content chemical screening to identify small molecules that can replace *Sox2* in reprogramming. We show that one of these molecules functions in reprogramming by inhibiting Tgf-β signaling in a stable and trapped intermediate cell type that forms during the process. We find that this inhibition promotes the completion of reprogramming through induction of the transcription factor *Nanog*.

INTRODUCTION

Retroviral transduction with three genes, *Sox2*, *Oct4*, and *Klf4*, can directly reprogram somatic cells to a pluripotent stem cell state (Okita et al., 2007; Takahashi et al., 2007b). Unfortunately, the resulting induced pluripotent stem cells (iPSCs) are suboptimal for applications in transplantation medicine and disease modeling because both the viral vectors used for gene transfer and the reprogramming factors they encode are oncogenic (Hacein-Bey-Abina et al., 2003; Nakagawa et al., 2008; Thrasher and Gaspar, 2007).

One potential solution is to identify small molecules that can efficiently reprogram cells and produce unmodified iPSC lines better suited for downstream applications as a result. Identification of such compounds would allow reprogramming that would not be impeded by the laborious nature of protein transduction or the safety concerns surrounding transgenic approaches (Kaji et al., 2009; Kim et al., 2009; Okita et al., 2008).

Several small molecules that catalyze reprogramming have already been described. Compounds that alter chromatin structure, including the DNA methyltransferase inhibitor 5-aza-cytidine (AZA) and the histone deacetylase (HDAC) inhibitor valproic acid (VPA), can increase reprogramming efficiency and even reduce the number of factors required for reprogramming (Huangfu et al., 2008a; Huangfu et al., 2008b; Mikkelsen et al., 2008; Shi et al., 2008b) . Treatment with these inhibitors presumably lowers the barrier to activation of endogenous pluripotency-associated genes. However, *Oct4* and *Sox2* not only activate genes required for pluripotency, they also function to repress genes promoting differentiation. It is therefore unlikely that this class of small molecules would be sufficient to completely replace the transgenic factors. As a result, there remains a need to identify novel small molecules that can function in reprogramming.

Here, we report the discovery of compounds that can replace the central reprogramming factor *Sox2*. We demonstrate that one of these chemicals specifically acts by inhibiting Tgf-β signaling. Interestingly, this compound does not act by inducing *Sox2* expression in the target fibroblasts. Instead, we show that it enables reprogramming through the induction of *Nanog* transcription in a stable, partially reprogrammed cell type that accumulates in the absence of *Sox2*.

RESULTS

A Screen for Chemical Mediators of Reprogramming

To identify small molecules that function in reprogramming, we transduced fibroblasts with viral vectors encoding *Oct4*, *Klf4*, and *cMyc* and then screened for compounds that allowed for reprogramming in the absence of *Sox2*. We favored this approach because it was unbiased with respect to the mechanism by which a given chemical could function and would not only deliver chemical compounds with translational utility but also provide novel insights into the mechanisms controlling reprogramming.

Activation of an *Oct4*::GFP reporter gene in colonies with an embryonic stem cell (ESC) morphology has been shown to be a stringent assay for reprogramming (Meissner et al., 2007). In
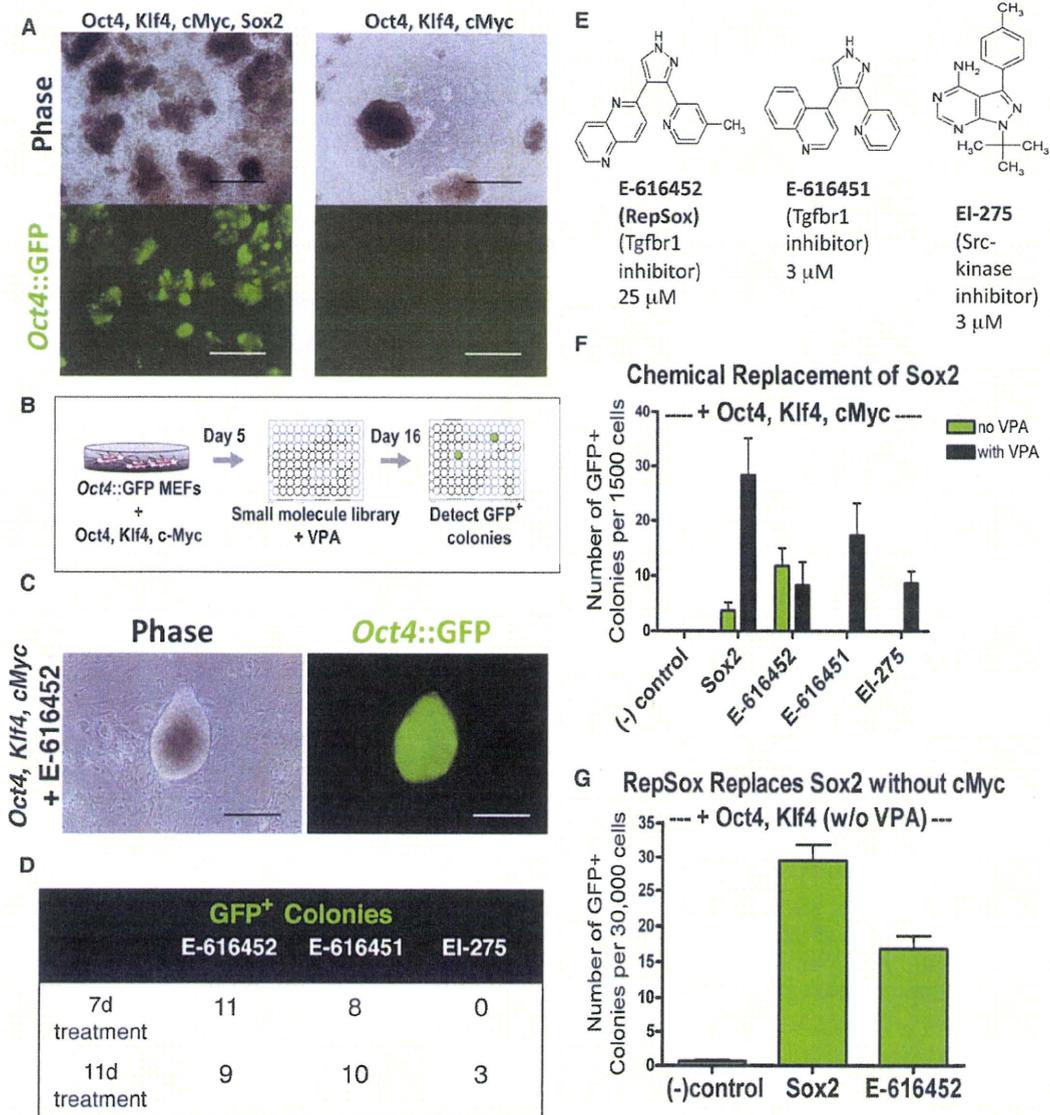
Figure 1. Identification of Small Molecules That Replace of *Sox2*

(A) *Oct4*::GFP⁺ colonies form readily in *Oct4*, *Klf4*, *cMyc*, and *Sox2*-infected MEF cultures and do not form in *Oct4*-, *Klf4*-, and *cMyc*-infected MEF cultures. Scale bars represent 500 μm.

(B) Overview of chemical screen for replacement of *Sox2*.

(C) A P0 colony from *Oct4*-, *Klf4*-, and *cMyc*-infected MEFs + RepSox that displays a mESC-like morphology and is *Oct4*::GFP⁺. Scale bars represent 200 μm.

(D) Number of *Oct4*::GFP⁺ colonies detected for each hit in the primary screen after transduction of *Oct4*, *Klf4*, and *cMyc* and VPA treatment.

(E) Chemical structures of E-616452, E-616451, and EI-275, with the optimal concentrations for reprogramming listed.

(F) Quantification of small-molecule replacement of *Sox2* in *Oct4*-, *Klf4*-, and *cMyc*-infected MEFs with and without VPA treatment. The error bars denote the standard error derived from quantification of three separate wells of cells.

(G) *Sox2* replacement by RepSox is not dependent on *cMyc* (no VPA treatment). The error bars denote the standard error derived from quantification of three separate wells of cells.

mouse embryonic stem cell (mESC) culture medium supplemented with VPA, retroviral transduction of 7500 *Oct4*::GFP transgenic mouse embryonic fibroblasts (MEFs) with *Oct4*, *Klf4*, *cMyc*, and *Sox2* (Boiani et al., 2004) routinely generated 100–200 GFP⁺ colonies (Figure 1A). In contrast, we observed no GFP⁺ colonies when *Sox2* was omitted (Figure 1A). We used this robust difference to identify small molecules that can replace *Sox2*.

To facilitate the identification of cellular targets and signaling pathways affected by any compounds we discovered, we utilized a library of molecules with known pharmacological targets. We transduced *Oct4*::GFP MEFs with *Oct4*, *Klf4*, and *cMyc* and

then plated 2000 cells per well in a 96-well format. To each well, we added one of 800 distinct compounds for 7–11 days and also treated each well with 2 mM VPA for the first 7 days (Figure 1B). It was our hope that this approach would allow us to identify both compounds that required chromatin remodeling to induce reprogramming (Huangfu et al., 2008a) and compounds that did not. After 16 days, we scored each well for the presence of GFP⁺ colonies with a mESC-like morphology (Figure 1C) and identified three independent hit compounds (Figure 1D). Two of these compounds were distinct transforming growth factor-β receptor 1 (Tgfbr1) kinase inhibitors (E-616452 and E-616451 [Figure 1E] [Gellibert et al., 2004]), whereas the third was a Src-family kinase inhibitor (EI-275 [Figure 1E] [Hanke et al., 1996]).

Efficient Small-Molecule Replacement of Sox2

Next, we optimized the effective concentration for each hit molecule (Figure S1 available online) and quantified the efficiency at which it synergized with VPA to replace *Sox2*. When 1500 MEFs were transduced with only *Oct4*, *Klf4*, and *cMyc* and then treated with VPA, we did not observe GFP⁺ colonies (Figure 1F). However, the addition of E-616452 (25 μM), E-616451 (3 μM), or EI-275 (3 μM) led to the formation of GFP⁺ colonies with an ESC morphology at a rate that was comparable to transduction with *Sox2* (Figure 1F).

Given that the three compounds were identified in the presence of VPA, we next determined whether these molecules were dependent on this HDAC inhibitor for their reprogramming activities. We found that E-616451 and EI-275 could not induce the appearance of GFP⁺ colonies in the absence of VPA (Figure 1F), whereas E-616452 could do so and at a rate that was similar to a positive control transduced with the *Sox2* retrovirus (Figure 1F).

Although *cMyc* does increase the efficiency of reprogramming, it is not required for the generation of iPSCs (Nakagawa et al., 2008). Because the elimination of *cMyc* is an important step toward reducing the risk of tumor formation, we tested whether E-616452 could function in the absence of this oncogene. When added to MEFs transduced with only *Oct4* and *Klf4*, E-616452 induced the formation of GFP⁺ colonies with an efficiency similar to viral *Sox2* (Figure 1G).

Previous reports on small molecules that affect reprogramming have focused on MEFs or neural stem cells (NSCs). These cells may be reprogrammed more easily because of either their proliferative capacity or their expression of iPSC factors (Huangfu et al., 2008a; Shi et al., 2008a; Shi et al., 2008b). However, it may be that chemical modulation of gene expression is cell-type specific, and we therefore determined whether the reprogramming compound we identified functioned in a more patient-relevant cell type. When we infected adult tail tip fibroblasts with *Oct4*, *Klf4*, and *cMyc* alone, we did not observe *Oct4*::GFP⁺ colonies. However, when we added E-616452, we readily observed reprogramming (Figure S2A). The resulting *Oct4*::GFP⁺ colonies could be expanded into cell lines that maintained homogeneous *Oct4*::GFP expression and self-renewed similarly to mESC and 4-factor control iPSC lines (Figure S2B). Because it could efficiently replace transgenic *Sox2* in the absence of VPA and *cMyc*, as well as in both embryonic and adult fibroblasts, we chose to further characterize E-616452 and named it RepSox, for Replacement of *Sox2*.

RepSox-Reprogrammed Cells Are iPSCs

Investigation of self-renewal capacity (Figure 2A), gene expression program, and pluripotency demonstrated that *Oct4*::GFP⁺ cells induced by the RepSox replacement of *Sox2* were bona fide iPSCs. PCR with primers specific to the *Oct4*, *Klf4*, *cMyc*, and *Sox2* transgenes confirmed that this cell line did not harbor transgenic *Sox2* (Figure S3A). Chromosomal analysis indicated it was karyotypically normal (Figure S3B).

The *Oct4*::GFP⁺ cells coexpressed alkaline phosphatase (Figure S3C) and the endogenous alleles of the *Nanog* and *Sox2* genes, suggesting pluripotency had been established (Figure 2B). The global transcriptional profile of cells reprogrammed with RepSox was similar to that of an iPSC line produced with all four transgenes and as similar to those of mESCs (Pearson correlation coefficient = 0.95–0.97) as two distinct mESC lines profiles were to each other (Pearson correlation coefficient = 0.96) (Figure 2C, Figure S3D, and Table S1). The profile differed significantly from that of the somatic MEFs (Figure 2C).

Cells produced with RepSox could readily form both embryoid bodies and teratomas that contained differentiated cell types of the three distinct embryonic germ layers (Figure 2E and Figure S4A). In addition, we observed that these cells could respond to directed differentiation signals in vitro and robustly differentiate into Hb9+/Tuj1+ motor neurons (Figure 2D and Figure S5).

In order to more definitively confirm the pluripotency of cells reprogrammed with RepSox, we tested their ability to contribute to chimeric embryos in vivo. We labeled cells with a lentiviral transgene encoding the dTomato red fluorescent protein and injected them into blastocysts. Both embryos and adult mice with significant contribution from the iPSCs were obtained (Figures 2F and 2G). Although adult mice with high contribution from the iPSCs were observed, we found it difficult to assess the contribution of these cells to the germline because the majority of animals developed tumors at or before the time of sexual maturity. However, we did observe that the reprogrammed cells could contribute *Oct4*::GFP⁺ cells to the genital ridges of embryonic chimeras, demonstrating contribution of these pluripotent cells to the germline (Figure 2H). Together, these results demonstrate that the RepSox-reprogrammed cells are indeed iPSCs.

RepSox Can Replace Sox2 and c-Myc by Inhibiting Tgf-β Signaling

Previous studies with RepSox suggest that it can act as an inhibitor of the Tgfbr1 kinase (Gellibert et al., 2004). Therefore, we investigated whether the mechanism by which RepSox functions to replace *Sox2* is through the inhibition of Tgf-β signaling. If Tgfbr1 is the functional target of RepSox, then a structurally unrelated inhibitor of Tgf-β signaling or depletion of Tgf-β ligands from the culture medium might also replace *Sox2*. The small molecule SB431542 (Figure 3A) is known to inhibit Tgfbr1 kinase and is structurally distinct from RepSox (Inman et al., 2002). When we treated fibroblasts transduced with *Oct4*, *Klf4*, and *cMyc* with 25 μM SB431542, we observed ~10 GFP⁺ colonies per 7500 cells plated (Figure 3B). Likewise, when we transduced fibroblasts in the presence of either an antibody that neutralized a variety of Tgf-β ligands (R&D Systems, AB-100-NA) or an antibody specific to Tgf-β II (R&D Systems, AB-12-NA), *Oct4*::GFP⁺ colonies were generated (Figure 3B). In contrast, we observed no GFP⁺ colonies in transductions without these Tgf-β inhibitors.
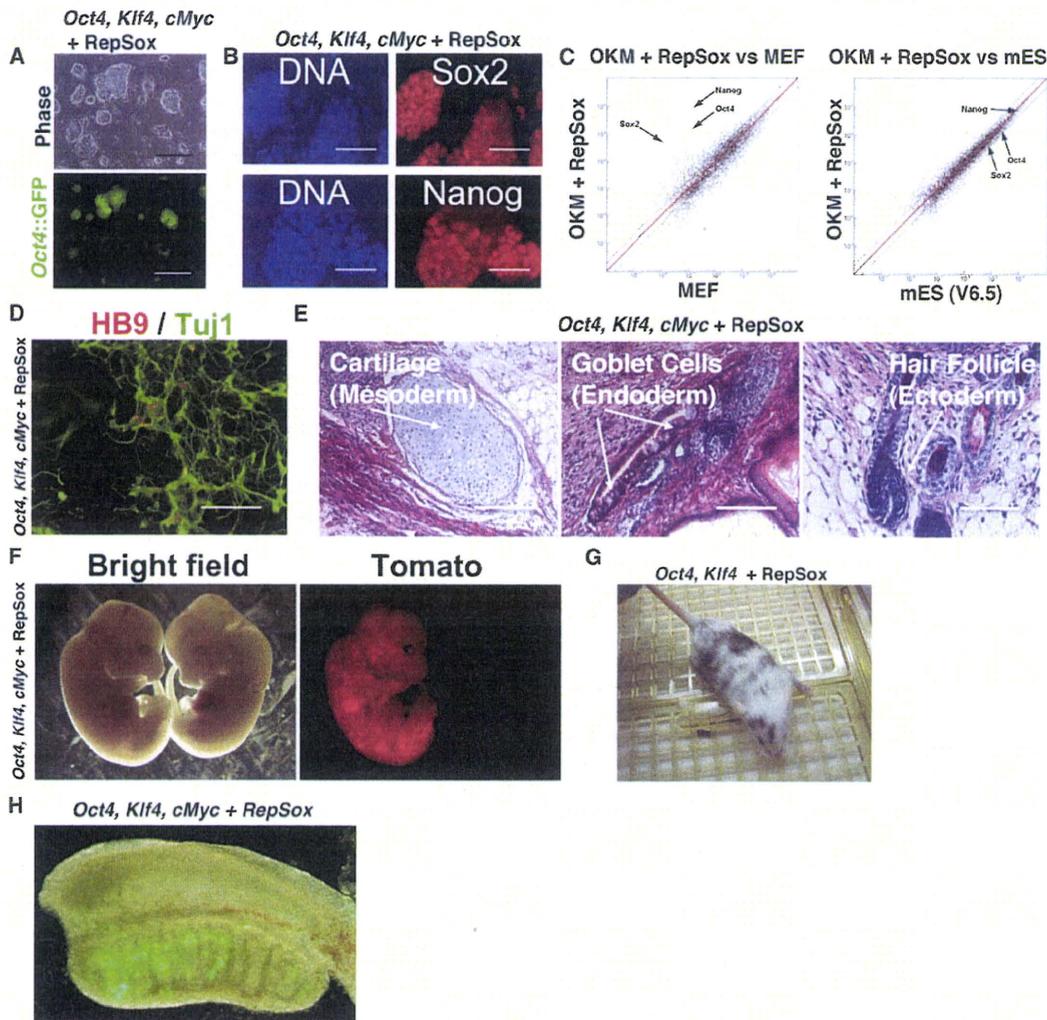
Figure 2. RepSox-Reprogrammed Cells Are Pluripotent

(A) An *Oct4*::GFP⁺ iPSC line that was derived from a culture of RepSox-treated *Oct4*, *Klf4*, and *cMyc*-infected MEFs (OKM + RepSox line 1) displays the characteristic mESC-like morphology and self-renewal properties. Passage 11 is shown. Scale bars represent 500 μm.

(B) Antibody staining of OKM + RepSox line 1 cells shows that they express markers of pluripotent stem cells Sox2 and Nanog. Scale bars represent 100 μm.

(C) Microarray scatter plots showing that the global gene expression profile of OKM + RepSox line 1 is highly similar to that of mESC line V6.5 and very different from that of somatic MEFs.

(D) Motor neurons differentiated in vitro from OKM + RepSox line 1. The scale bar represents 200 μm.

(E) Teratomas containing cells of all three germ layers formed by injection of OKM + RepSox line 1 cells into nude mice.

(F) E12.5 chimeric mouse embryo (left, versus nonchimeric littermate on the right) showing a high amount of contribution from OKM + RepSox line 1 cells constitutively expressing the dTomato red fluorescent protein.

(G) Eight-week-old chimeric mouse formed by injection of OK + RepSox line 1 cells (C57BL6 genetic background) into an ICR blastocyst.

(H) *Oct4*::GFP⁺ cells derived from an OKM + RepSox cell line are present in the genital ridge of a male embryo at 13.5 days postcoitum (dpc).

These results are consistent with the notion that at least part of the mechanism by which RepSox replaces *Sox2* in reprogramming is through the inhibition of Tgf-β signaling.

Our goal was to identify molecules that specifically replace *Sox2* instead of generally increasing reprogramming efficiency. If RepSox acts specifically to replace *Sox2*, then we would not expect it to stimulate reprogramming in the presence of transgenic *Sox2*. When RepSox- or Tgf-β antibody-treated MEFs were transduced with *Oct4*, *Klf4*, *cMyc*, and *Sox2*, we observed

less than a 2-fold increase in the number of GFP⁺ colonies over the untreated controls (Figures 3C and 3D). The magnitude by which RepSox stimulated reprogramming in this context was significantly less than the 10-fold increase that we observed after treatment with VPA, a compound thought to increase reprogramming efficiency (Figure 1F).

In order to further investigate the specificity of *Sox2* replacement by RepSox, we tested the ability of this molecule to individually replace *Oct4*, *Klf4*, and *cMyc* in reprogramming. We found
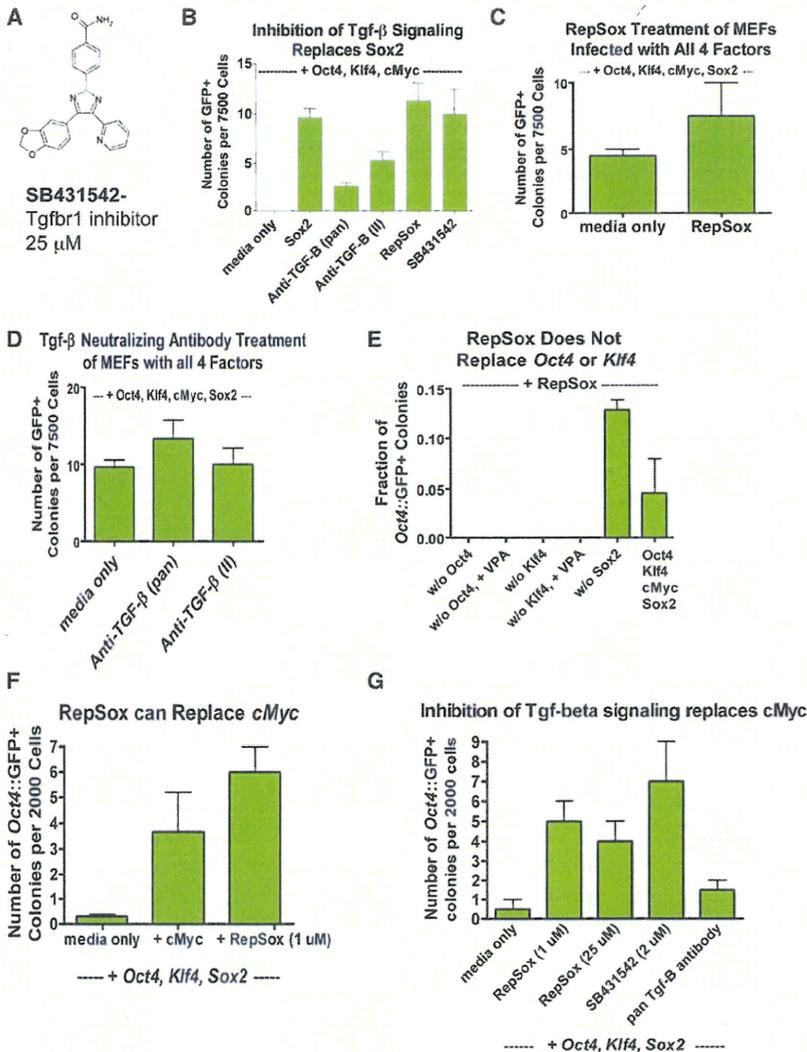
Figure 3. RepSox Specifically Replaces *Sox2* by Inhibiting Tgf-β Signaling

(A) Chemical structure of SB431542, an inhibitor of Tgfbr1 activity.

(B) Inhibition of Tgf-β signaling by treatment of *Oct4-*, *cMyc-*, and *Sox2*-infected MEFs with SB431542 or TGF-β neutralizing antibodies replaces *Sox2*.

(C) RepSox does not increase the efficiency of *Oct4*::GFP⁺ colony induction in *Oct4-*, *Klf4-*, *cMyc-*, and *Sox2*-infected MEFs. The error bars denote the standard error derived from quantification of three separate wells of cells.

(D) Inhibition of Tgf-β signaling by TGF-β neutralizing antibodies does not increase the efficiency of *Oct4*::GFP⁺ colony induction in *Oct4-*, *Klf4-*, *cMyc-*, and *Sox2*-infected MEFs. The error bars denote the standard error derived from quantification of three separate wells of cells.

(E) RepSox does not replace transgenic *Oct4* or transgenic *Klf4* in reprogramming. We observed no *Oct4*::GFP⁺ colonies in RepSox-treated *Klf4-*, *cMyc-*, and *Sox2*-infected MEFs or *Oct4-*, *cMyc-*, *Sox2*-infected MEFs out of 30,000 cells plated both with and without VPA treatment. We routinely observe 30–40 *Oct4*::GFP⁺ colonies when we plate the same number of *Oct4-*, *Klf4-*, and *cMyc*-infected MEFs and treat them with RepSox. The error bars denote the standard error derived from quantification of three separate wells of cells.

(F) RepSox can replace *cMyc* in reprogramming. Cells were transduced with *Oct4*, *Klf4*, and *cMyc* and treated with RepSox continuously starting at day 5 postinfection. The error bars denote the standard error derived from quantification of two separate wells of cells.

(G) Inhibition of Tgf-β signaling can replace *cMyc* in reprogramming. Cells were transduced with *Oct4*, *Klf4*, and *cMyc* and treated with inhibitors of Tgf-β signaling continuously starting at day 5 postinfection. The error bars denote the standard error derived from quantification of two separate wells of cells.

that RepSox could not induce GFP⁺ colonies in the absence of either *Oct4* or *Klf4*, even in the presence of VPA (Figure 3E). In contrast, we found that RepSox did increase the number of *Oct4*::GFP⁺ colonies by 20-fold in the absence of *cMyc*, thereby fully replacing it in reprogramming (Figure 3F). In addition, the structurally distinct Tgf-β inhibitor SB431542 and a Tgf-β-specific neutralizing antibody both increased reprogramming efficiency in the absence of *cMyc* (Figure 3G). From these experiments, we conclude that RepSox enables the replacement of the reprogramming activities provided by both transgenic *Sox2* and *cMyc*. In both cases, these complementing activities seem to be mediated through the inhibition of Tgf-β signaling.

RepSox Replaces *Sox2* by Acting on Intermediates Formed During the Reprogramming Process

The development of cocktails of small molecules that can effectively reprogram somatic cells may require a detailed knowledge of the mechanism and kinetics by which each compound acts. Therefore, we determined the optimal duration of time by which

inhibition of Tgf-β signaling with RepSox can help induce reprogramming.

Initially, we pretreated MEFs with RepSox, applying the chemical for 3 days, and then removed it at the time of transduction with *Oct4*, *Klf4*, and *cMyc*. In these experiments, no *Oct4*::GFP⁺ colonies were formed (Figure 4A), suggesting that RepSox does not act on the initial somatic cells to replace *Sox2*. Consistent with this result, we did not detect a significant increase in the expression of endogenous *Sox2* or closely related *Sox* family members upon RepSox treatment (Figure S6A). In addition, RepSox treatment did not decrease the expression of the mesenchymal gene *Snai1* (Figure S6B), which is downregulated 5- to 40-fold by transduction of the four reprogramming factors (Mikkelsen et al., 2008). Thus, RepSox does not destabilize the pre-existing MEF transcriptional program.

In contrast, we found that RepSox did increase by 5-fold the expression of *L-Myc*, a close homolog of *cMyc* that can functionally replace it in reprogramming (Nakagawa et al., 2008) (Figure S6C). Together, these data suggest that although RepSox
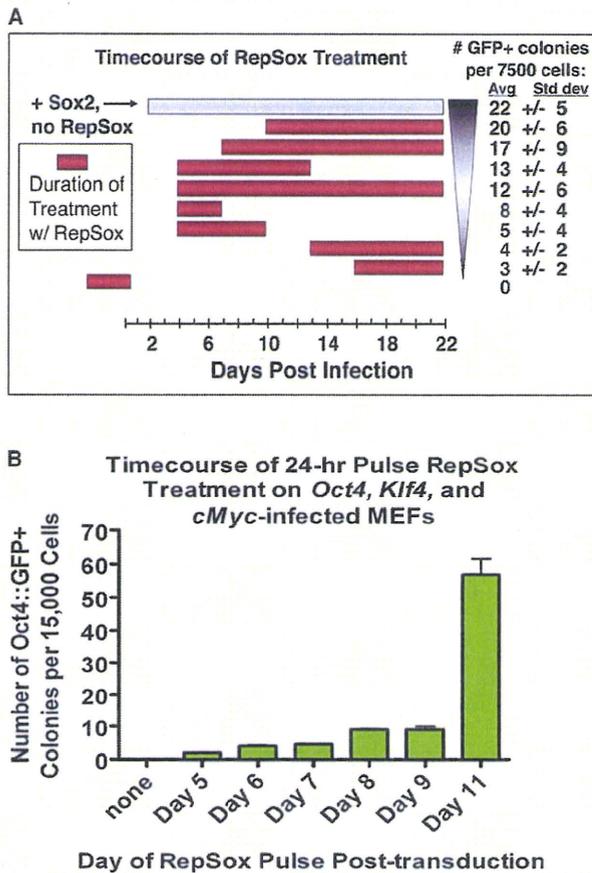
A

B

Figure 4. A Short Pulse of RepSox Is Sufficient for *Sox2* Replacement and Most Effective at Later Time Points after Infection

(A) Graph showing the number of *Oct4*::GFP+ colonies induced by various timings of RepSox treatment of *Oct4*-, *Klf4*-, and *Sox2*-infected MEFs in mESC medium. Colonies were counted at 24 days postinfection. Shown are average colony numbers ± the standard deviation. The standard deviation was derived from quantification of two separate wells.

(B) Time course of RepSox treatment showing the number of *Oct4*::GFP+ colonies induced by a 24 hr pulse of RepSox on *Oct4*-, *Klf4*-, and *Sox2*-infected MEFs in serum-free mESC medium with knockout serum replacement (KSR mESC). Colonies were counted at 24 days postinfection. The error bars denote the standard error derived from quantification of three separate wells of cells.

probably functions at the level of the initial somatic cell population to replace *cMyc*, it does not act on the starting MEF population to replace *Sox2*.

Because RepSox did not seem to act directly on the fibroblasts to replace *Sox2*, we investigated whether it functioned on intermediates that arose during reprogramming. To address this question, we varied both the duration and timing of RepSox treatment in order to determine when it was most effective. First, we transduced 7500 MEFs with *Oct4*, *Klf4*, and *cMyc*, waited for 4 days, and subsequently treated cultures with RepSox for 3, 6, 9, or 18 additional days. Although a short 3 day treatment from days 4–7 induced a small number of *Oct4*::GFP+ colonies, the 9-day treatment from days 4–13 yielded the most *Oct4*::GFP+ colonies (Figure 4A).

Next, we varied the timing at which we initiated RepSox treatment, by administering the compound beginning at day 4, 7, 10, 13, or 16 after transduction. We found that delaying the start of RepSox treatment increased its reprogramming potency, with optimal treatment beginning at 10 days posttransduction (Figure 4A). Together, these results suggest that RepSox treatment is most effective between days 7–12 posttransduction.

To more precisely define the optimal treatment window, we determined the minimal duration of treatment required to induce reprogramming. We found that a treatment as short as only 1 day was sufficient for inducing detectable reprogramming (Figure 4B). Delaying this short treatment yielded more reprogrammed colonies, with a sharp increase at day 11 (Figure 4B). These results indicate that RepSox is most effective at replacing *Sox2* during days 10–11 after transduction and that therefore cultures of *Oct4*, *Klf4*, and *cMyc*-transduced MEFs give rise to intermediates capable of responding to RepSox treatment. These intermediates appear at day 4 posttransduction and peak at days 10–11.

Interestingly, when we tracked the timing of the initial appearance of reprogrammed colonies as a function of the timing of RepSox administration, we found that regardless of whether we began treatment at day 7 or day 10 posttransduction, *Oct4*::GFP+ colonies first appeared at day 14 (Figure S7). This suggests that RepSox may not always be the rate-limiting step in this reprogramming process and that other, RepSox-independent events take place during the formation of the RepSox-responsive intermediates.

RepSox-Responsive Cell Lines

Our finding that a 24 hr pulse of RepSox can replace *Sox2* (Figure 4B) differs strikingly from the 5–10 day period of transgene expression normally required (Sridharan et al., 2009; Wernig et al., 2007) and suggests that RepSox could trigger a switch activating reprogramming. If RepSox acts to flip a switch in semi-stable intermediate cell types that accumulate in the absence of retroviral *Sox2* expression, we reasoned that it might also be possible to culture these responsive intermediates for prolonged periods of time. In contrast, if RepSox acts during a critical window on very transient intermediates, this might not be possible. To distinguish between these models, we transduced *Oct4*::GFP MEFs with *Oct4*, *Klf4*, and *cMyc*, waited 10-14 days, and subsequently clonally expanded ten iPSC-like, GFP-negative colonies (Figure 5A). These cell lines continued to proliferate for at least four passages and often maintained an iPSC-like morphology (Figure 5A), but never further activated expression of *Oct4*::GFP. However, when we treated these cell lines with a 48 hr pulse of RepSox, 5%–10% of the colonies in two of the ten lines became *Oct4*::GFP+ (Figures 5A and 5B). These results demonstrate that partially reprogrammed cells can accumulate in the absence of *Sox2* and that some, but not all, of these cells can be clonally expanded and cultured for prolonged periods while maintaining responsiveness to RepSox.

As we had shown that this particular reprogramming molecule seems to replace *Sox2* through the inhibition of Tgf-β signaling, we sought to determine whether RepSox treatment affected Tgf-β signal transduction pathways in these responsive cell lines. To this end, we determined the levels of phosphorylated Smad3 by western blotting in cell line OKM 10 both with and without
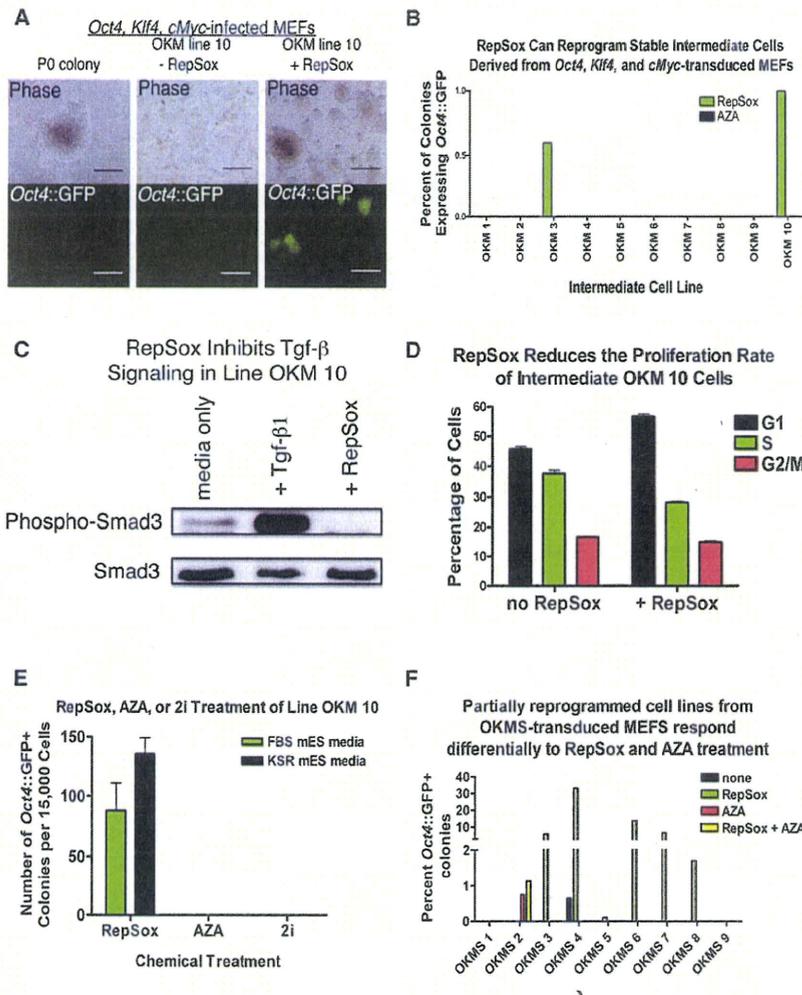
A

B

C

D

E

F

Figure 5. Stable Intermediates Can Be Reprogrammed by RepSox

(A) Stable *Oct4*::GFP-negative cell lines derived from *Oct4*::GFP-negative colonies in *Oct4*-, *Klf4*-, and *cMyc*-infected MEF cultures can be reprogrammed by RepSox. Scale bars in "OKM line 10 + RepSox" panels represent 500 μm; all other scale bars represent 200 μm.

(B) Two of ten stable, nonpluripotent intermediate cell lines derived from MEFs transduced with *Oct4*, *Klf4*, and *cMyc* can be reprogrammed with RepSox treatment, but none can be reprogrammed with AZA treatment.

(C) Western blot for phospho-Smad3 showing that RepSox inhibits Tgf-β signaling in line OKM 10 (OKM 10) cells.

(D) RepSox does not increase the proliferation of OKM 10 cells. The error bars denote the standard error derived from quantification of two separate wells of cells.

(E) Line OKM 10 can be reprogrammed with RepSox treatment but not with AZA or 2i, indicating it is distinct from cell lines that can be reprogrammed by AZA or 2i. The error bars denote the standard error derived from quantification of three separate wells of cells.

(F) Stable *Oct4*::GFP-negative cell lines derived from *Oct4*::GFP-negative colonies in *Oct4*-, *Klf4*-, *cMyc*-, and *Sox2*-infected MEF cultures can be reprogrammed by RepSox or by AZA, but lines responsive to RepSox are not responsive to AZA alone and lines responsive to AZA are not responsive to RepSox alone, indicating the presence of two different types of stable intermediates in the reprogramming cultures.

RepSox treatment. Without RepSox treatment, we detected relatively high levels of phosphorylated Smad3, suggesting that Tgf-β signaling was active (Figure 5C). In contrast, treatment with 25 μM RepSox almost completely eliminated Smad3 phosphorylation (Figure 5C), indicating that RepSox strongly inhibited Tgf-β signaling in these cells.

Because an increase in cell proliferation can also increase reprogramming efficiency (Hong et al., 2009) and possibly contribute to the replacement of transgenic *Sox2*, we measured the proliferation rate of partially reprogrammed OKM 10 cells both with and without RepSox. Treatment with RepSox decreased the proportion of cells in G2/M phase of the cell cycle (Figure 5D), indicating it does not increase the proliferation rate of these partially reprogrammed cells.

Cells that Respond to RepSox Treatment Are Distinct from Previously Described Intermediates

It has been shown that certain nonpluripotent, partially reprogrammed cell lines derived from MEFs transduced with *Oct4*, *Klf4*, *cMyc*, and *Sox2* can be fully reprogrammed with AZA or a combination of chemical inhibitors of glycogen synthase kinase 3β (GSK-3β) and the Mek signaling pathway (2i conditions)

(Mikkelsen et al., 2008; Silva et al., 2008). If the RepSox-responsive cell lines generated by overexpression of *Oct4*, *Klf4*, and *cMyc* are similar to these four-factor cell lines, then they should also be reprogrammed by AZA or 2i. However, when we treated the ten stable intermediate lines with either AZA or 2i for 48 hr, we found that none became reprogrammed (Figure 5B), indicating that the RepSox-responsive stable intermediates are distinct from partially reprogrammed cell lines described previously (Mikkelsen et al., 2008; Silva et al., 2009). Consistent with these results, in vitro assays of kinase activity revealed that RepSox does not inhibit the targets of the 2i cocktail (Table S2).

It occurred to us that some nonpluripotent cells derived from MEFs transduced with *Oct4*, *Klf4*, *cMyc*, and *Sox2* could potentially be held in a nonpluripotent state because of inappropriate levels of transgene expression and therefore might also be responsive to RepSox treatment. To test this hypothesis, we transduced *Oct4*::GFP MEFs with *Oct4*, *Klf4*, *cMyc*, and *Sox2*, then picked and clonally expanded nine GFP-negative colonies at day 14 after transduction (Figure S8). After treatment with RepSox, five of the nine cell lines yielded reprogrammed colonies, with 2%–33% of the colonies in each line becoming *Oct4*::GFP+ (Figure 5F and Figure S8). These results indicate
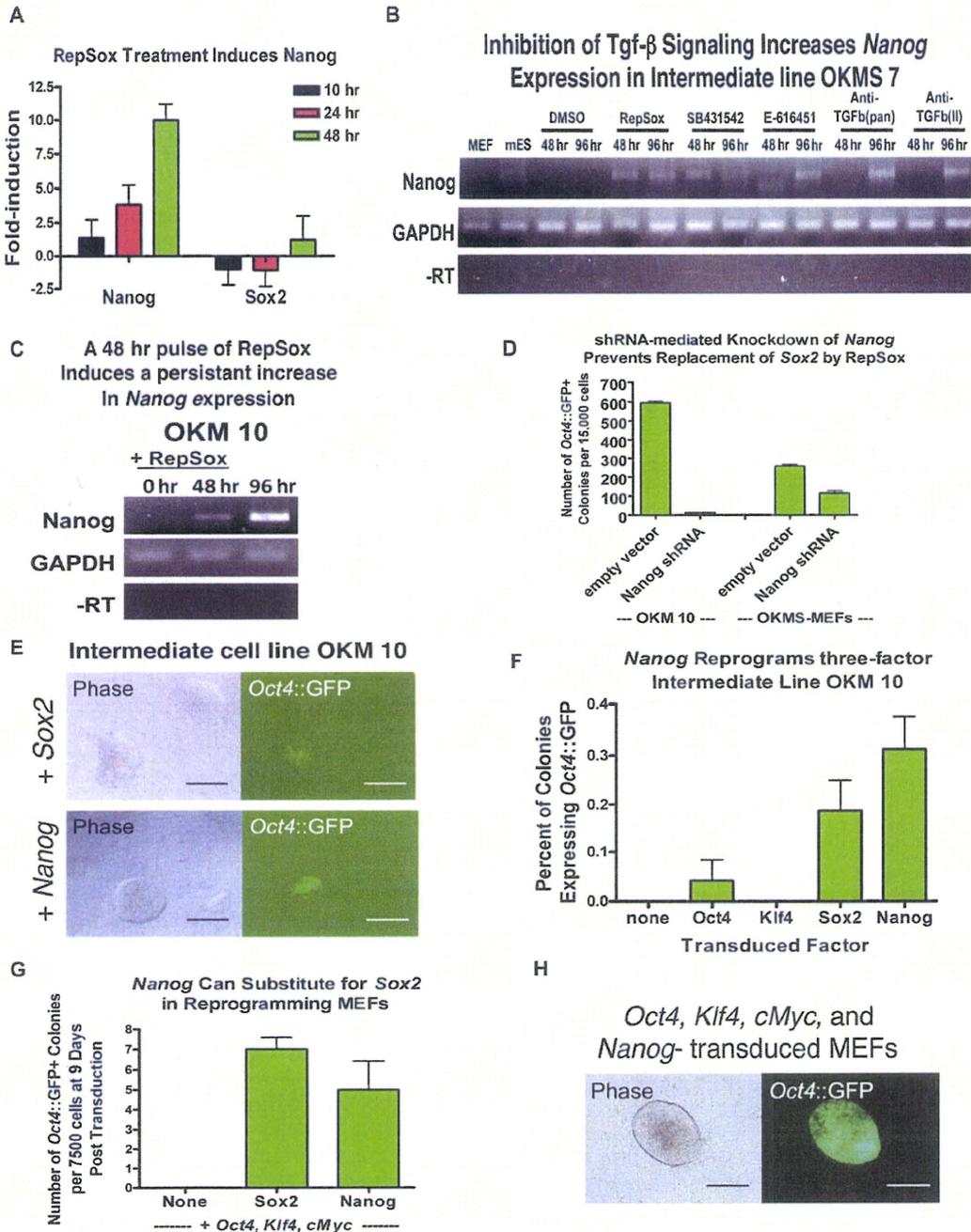
Figure 6. RepSox Replaces *Sox2* by Inducing *Nanog* Expression

(A) RepSox treatment of RepSox-responsive line OKMS 6 strongly increases *Nanog* mRNA levels. Data were generated by microarray analysis and are relative to untreated controls. *Nanog* is induced more quickly and more significantly than *Sox2*, indicating it is upregulated before fully reprogrammed cells form. The error bars denote the standard error derived from quantification of three separate wells of cells.

(B) RT-PCR analysis showing that inhibition of Tgf-β signaling increases *Nanog* expression in the RepSox-responsive intermediate line OKMS 7.

(C) A pulse of RepSox induces a persistent increase in *Nanog* expression in the RepSox-responsive intermediate line OKM 10. OKM 10 cells were treated with 25 µM RepSox for 48 hr and RNA samples were taken at 0, 48, and 96 hr (48 hr after removal of RepSox) and analyzed by RT-PCR.

(D) shRNA-mediated knockdown of *Nanog* in OKM 10 cells inhibits replacement of *Sox2* by RepSox. The error bars denote the standard error derived from quantification of two separate wells of cells.

(E) Pictures of reprogrammed *Oct4*::GFP+ colonies induced by *Sox2* (A) or *Nanog* (B) transduction of line OKM 10. Scale bars represent 200 µm.

(F) *Nanog* transduction can reprogram line OKM 10 at an efficiency similar to that of *Sox2* transduction. The error bars denote the standard error derived from quantification of three separate wells of cells.

that like the stable intermediate cells generated with only *Oct4*, *Klf4*, and *cMyc*, certain incompletely reprogrammed cells generated by *Oct4*, *Klf4*, *cMyc*, and *Sox2* transduction can also be reprogrammed by RepSox.

Next, in order to determine whether these RepSox-responsive intermediate cell lines derived after *Oct4*, *Klf4*, *cMyc*, and *Sox2* transduction were similar to or distinct from previously described partially reprogrammed cell lines (Mikkelsen et al., 2008), we applied AZA to all nine lines. After 48 hr of AZA treatment and 12 subsequent days in culture, none of the RepSox-responsive cell lines expressed *Oct4*::GFP (Figure 5F). However, one of the lines that had been refractory to RepSox treatment did express *Oct4*::GFP after AZA treatment, indicating that it had undergone complete reprogramming (Figure 5F). Together, these results show that there are a variety of intermediates that can form after retroviral transduction and that they vary in their responsiveness to reprogramming molecules.

RepSox Replaces *Sox2* by Inducing *Nanog* Expression

The causal molecular events that drive reprogramming are difficult to detect because of the low efficiency at which somatic cells are successfully reprogrammed (Amabile and Meissner, 2009). However, when we administered RepSox to cell lines that had been partially reprogrammed by retroviral transduction, *Oct4*::GFP expression was induced in up to 33% of the resulting colonies (Figure 5F). We used this more efficient reprogramming system to identify the changes in gene expression induced by RepSox that enable it to bypass the requirement for transgenic *Sox2* expression.

We treated an *Oct4*::GFP-negative, partially reprogrammed cell line (OKMS 6) with RepSox and performed global gene expression analysis at 10, 24, and 48 hr after the initiation of treatment. To confirm that RepSox was inhibiting Tgf-β signaling in this intermediate cell line, we investigated expression changes in known Tgf-β-responsive genes after RepSox treatment. The *Inhibition of Differentiation* genes *Id1*, *Id2*, and *Id3* are repressed by Tgf-β signaling in mESCs (Ying et al., 2003). After treating the RepSox-responsive intermediate line OKM 10 with RepSox for 24 hr, we observed increased expression of *Id1*, *Id2*, and *Id3* (Figure S9A).

One way that RepSox could function to replace transgenic *Sox2* would be to induce the expression of endogenous *Sox2* or a *Sox* family member, such as *Sox1* or *Sox3*, that can substitute for it in reprogramming (Nakagawa et al., 2008). However, we again did not observe a significant increase in the expression of *Sox1*, *Sox2*, *Sox3*, or any of the remaining *Sox* family transcription factors within the first 48 hr of RepSox treatment (Figure S9B). Additionally, shRNA-mediated depletion of *Sox1*, the most potent *Sox* family member other than *Sox2* itself (Nakagawa et al., 2008), did not affect the rate of reprogramming in the presence of RepSox (Figure S9C). These results show that RepSox does not replace *Sox2* by directly activating endogenous *Sox2* or other closely related genes.

Next, we more broadly investigated changes in transcription factor expression after chemical treatment. We did not observe

an increase in endogenous *Oct4* or *Klf4* expression at early time points after RepSox treatment. However, we found that the expression of the homeodomain factor *Nanog* was among the most increased after RepSox treatment. Relative to untreated controls, *Nanog* transcription increased 4-fold within 24 hr and 10-fold after 48 hr of RepSox treatment (Figure 6A). In contrast, we did not observe a rapid increase in *Nanog* expression in two *Oct4*::GFP-negative intermediate cell lines that could not be fully reprogrammed with RepSox (Figure S10). Therefore, we hypothesized that RepSox might replace *Sox2* by inducing *Nanog* expression.

Because we had determined that inhibition of Tgf-β signaling by several different small molecules and antibodies can replace *Sox2*, we reasoned that if the increase in *Nanog* expression was critical for *Sox2* replacement, the alternative inhibitors of Tgf-β signaling should also upregulate *Nanog*. To test this hypothesis, we treated the RepSox-responsive cell lines with RepSox, SB431542, or neutralizing antibodies and analyzed *Nanog* expression after 48 hr. In all cases, *Nanog* expression was strongly induced within 48–96 hr (Figure 6B).

If RepSox functions by increasing *Nanog* expression, then a short pulse of RepSox should induce a persistent increase in *Nanog* expression. To test this, we treated the RepSox-responsive intermediate cell line OKM 10 with RepSox for 48 hr, withdrew RepSox, and analyzed *Nanog* expression 48 hr later. A control time point taken just before RepSox withdrawal showed a significant increase in *Nanog* transcription (Figure 6C). Forty-eight hours after RepSox removal (96 hr after the initiation of treatment), *Nanog* expression continued to increase (Figure 6C).

If RepSox replaces *Sox2* by increasing *Nanog* expression, then a forced reduction of *Nanog* expression should inhibit or even prevent reprogramming by RepSox. To test this hypothesis, we transduced the RepSox-responsive cell line with a lentivirus encoding a short-hairpin RNA specific for *Nanog*. The *Nanog*-knockdown cells reprogrammed at a frequency that was 50-fold lower than cells transduced with an empty control vector (Figure 6D). This effect was not caused by a general decrease in reprogramming efficiency or differentiation of reprogrammed cells due to *Nanog* depletion because MEFs transduced with *Oct4*, *Klf4*, *cMyc*, *Sox2*, and the *Nanog* shRNA construct only suffered a 50% loss in reprogramming efficiency (Figure 6D). These results demonstrate that increased *Nanog* expression in this context was only necessary for the replacement of *Sox2* by RepSox.

Previous reports have shown that chemical inhibition of Tgf-β signaling by SB431542 increases bone morphogenetic protein (Bmp) signaling in embryonic stem cells (Xu et al., 2008). It has separately been shown that Bmp signaling in the presence of Stat3 induces *Nanog* expression in mESCs (Suzuki et al., 2006). The crosstalk between the Tgf-β and Bmp signaling pathways may be the result of a common requirement for Smad 4, which mediates transcriptional events in the nucleus (Attisano and Wrana, 2002). Similarly, we observed an increase in the levels of phosphorylated Smad1 protein and *Bmp-3* mRNA in incompletely reprogrammed intermediates after RepSox

---

(G) *Nanog* can substitute for *Sox2* in defined-factor reprogramming of somatic fibroblasts. The error bars denote the standard error derived from quantification of three separate wells of cells.

(H) Picture of a reprogrammed *Oct4*::GFP+ colony induced by *Oct4*, *Klf4*, *cMyc*, and *Nanog* transduction of MEFs. Scale bars represent 100 μm.

treatment (Figure S11). Furthermore, the stable, partially reprogrammed cells that responded to RepSox expressed the LIF receptor at levels equivalent to those found in mESCs (Figure S12A). Expression of this receptor suggests that its downstream signal transduction pathway could be active in these cells, thereby resulting in the presence of activated Stat3, which is known to induce *Nanog* expression in conjunction with Bmp signaling.

Because RepSox does not act on the initial population of fibroblasts to replace *Sox2*, we would not expect *Nanog* to be upregulated in RepSox-treated MEFs. Indeed, within 7 days of transduction of MEFs with *Oct4*, *Klf4*, and *cMyc*, we did not observe an increase in *Nanog* expression upon RepSox treatment (Figure S12B). This may be explained in part by the observation that the LIF receptor, and thus activated Stat3, was not highly expressed in these cells (Figure S12A). Because *Nanog* plays a key role in maintaining ESCs in an undifferentiated state (Chambers et al., 2003) and has been shown to enhance the efficiency of reprogramming (Silva et al., 2006; Silva et al., 2009; Yu et al., 2007), we decided to test whether *Nanog* could directly replace *Sox2* in reprogramming.

If RepSox replaces *Sox2* by inducing *Nanog* expression, then retroviral transduction of RepSox-responsive intermediate cells (line OKM 10, Figures 5A and 5B) with *Nanog* should reprogram them. When we transduced line OKM 10 with *Sox2* as a control, 0.2% of the colonies expressed *Oct4*::GFP after 10 days, indicating that reprogramming could be induced in this cell line by *Sox2* (Figures 6E and 6F). When we transduced the same stable intermediate cell line with *Nanog*, it could also be reprogrammed, with 0.3% of the colonies expressing *Oct4*::GFP⁺ after 10 days (Figures 6E and 6F). In contrast, transductions with *Oct4* or *Klf4* resulted in only 0.04% and 0% reprogramming efficiencies (Figure 6F). These results suggest that *Nanog* can indeed functionally replace *Sox2* and induce reprogramming in these stable intermediates formed from *Oct4-*, *Klf4-*, and *cMyc*-transduced MEFs.

If *Nanog* can compensate for the omission of *Sox2* in defined-factor reprogramming, then MEFs transduced with *Oct4*, *Klf4*, *cMyc*, and *Nanog* might be as efficiently reprogrammed as MEFs transduced with *Oct4*, *Klf4*, *cMyc*, and *Sox2*. When we transduced MEFs with *Oct4*, *Klf4*, *cMyc*, and *Sox2* and scored cultures 9 days later, an average of seven *Oct4*::GFP⁺ colonies appeared for every 7500 cells plated (Figure 6G). A control transduction with only *Oct4*, *Klf4*, and *cMyc* yielded no *Oct4*::GFP⁺ colonies (Figure 6G). Similar to the positive control transduction, MEFs transduced with *Oct4*, *Klf4*, *cMyc*, and *Nanog* gave rise to an average of five *Oct4*::GFP⁺ colonies for every 7500 cells plated (Figures 6G, H). These colonies could be picked and expanded and remained *Oct4*::GFP⁺ for at least five passages (Figure S13A). Immunocytochemistry indicated that these cells strongly activated *Sox2* expression from the endogenous allele (Figure S13B). Importantly, QPCR analysis demonstrated that they also transcribed endogenous *Oct4*, *Klf4*, *Nanog*, and *Rex1* (Figure S13C), indicating that a pluripotent gene expression program had been established. Furthermore, transgene-specific QPCR analysis showed that these cells had silenced the retroviral *Oct4*, *Klf4*, and *cMyc* transgenes (Figure S13D). Additionally, *Oct4-*, *Klf4-*, *cMyc-*, and *Nanog*-reprogrammed cells could readily form embryoid bodies in vitro (Figure S13E). However,

we found that leaky expression of transgenic *Nanog*, which is a potent inhibitor of ESC differentiation (Chambers et al., 2003; Chambers et al., 2007), reduced the amount of differentiation in vitro (Figure S13D). We anticipate that efficient differentiation of cells created with *Oct4*, *Klf4*, *cMyc*, and *Nanog* will eventually require the use of an excisable transgenic *Nanog* cassette to completely remove ectopic *Nanog* expression. Although definitive proof of the pluripotency of these cells will be required to conclude that *Nanog* expression is sufficient for replacing *Sox2* in defined factor reprogramming, our results suggest that this may be the case. Taken together, our results demonstrate that RepSox inhibition of Tgf-β signaling bypasses the need for *Sox2* in defined-factor reprogramming through the induction of *Nanog*.

DISCUSSION

We have used a phenotypic chemical screen to identify compounds that can replace the reprogramming transcription factor *Sox2* and have confirmed the mechanism by which the most potent compound acts: RepSox replaces *Sox2* by inhibiting the broadly expressed Tgf-β signaling pathway (Attisano and Wrana, 2002) in cultures containing stable intermediate cells that are trapped in a partially reprogrammed state. This inhibition in turn leads to sustained transcription of *Nanog*, through which reprogramming is achieved in the absence of *Sox2*. These results demonstrate the feasibility of replacing the central reprogramming transgenes with small molecules that modulate discrete cellular pathways or processes rather than by globally altering chromatin structure. Furthermore, they show that the mechanisms by which these molecules act in reprogramming can be distinct from those of the factor(s) that they replace.

Importantly, and unlike many other studies (Mikkelsen et al., 2008; Shi et al., 2008a; Shi et al., 2008b; Utikal et al., 2009), the approach that we report here for replacing *Sox2* did not rely on procurement of a highly specialized or rare cell type that already expresses *Sox2*. Furthermore, treatment with RepSox allowed the generation of iPSCs from both adult and embryonic fibroblasts with a frequency comparable to that of transduction with *Sox2*. Thus, reprogramming efficiency does not need to be compromised by small-molecule replacement of transgenic factors.

We observed that instead of working on the initial fibroblast population to replace *Sox2*, RepSox acts on cellular intermediates formed by overexpression of *Oct4*, *Klf4,* and *cMyc*. Without RepSox treatment, these intermediates are trapped in an unproductive state. Unlike previously described partially reprogrammed cells (Mikkelsen et al., 2008; Silva et al., 2009), the RepSox-responsive intermediates could not be reprogrammed with AZA or 2i treatment, suggesting that they are distinct. In addition, we found that RepSox does not target any of the kinases inhibited by the 2i cocktail, indicating that it works through a different mechanism. Furthermore, four-factor intermediates that reprogram with RepSox treatment are not responsive to AZA, indicating that they also are distinct.

These findings demonstrate that reprogramming can proceed in a stepwise fashion through different intermediates. Just as in a geographical setting in where there are multiple routes to travel from point A to point B, there exist different intermediate states

or "way stations" that somatic cells can transit through on the way to complete reprogramming. Interestingly, although our results indicate that defined-factor reprogramming with *Oct4*, *Klf4*, *cMyc*, and *Sox2* can occur in the absence of *Nanog*, its induction is required for chemical reprogramming of both our RepSox-responsive intermediates and the recently described 2i-responsive intermediates made from *Oct4*, *Klf4*, and *cMyc* transduction of cells that express *Sox2* endogenously (Silva et al., 2009). This indicates that commonalities can exist in the reprogramming routes used by some sets of distinct intermediates.

Originally, we found it surprising that *Nanog* was not included in the initial set of defined reprogramming factors (Takahashi and Yamanaka, 2006) given its critical role in maintaining pluripotency in ESCs (Boyer et al., 2005; Chambers et al., 2003) and its ability to stimulate reprogramming by cell fusion (Silva et al., 2006). However, Takahashi and Yamanaka reported that a combination of nine factors that included *Oct4*, *Klf4*, *cMyc*, and *Nanog*, but not *Sox2*, generated iPSC colonies at a detectable rate (Takahashi and Yamanaka, 2006). This combination of factors included other genes that may have inadvertently lowered the rate of reprogramming, thereby causing the combination of *Oct4*, *Klf4*, *cMyc*, and *Nanog* to be overlooked. Consistent with these data, work by Niwa and coworkers with inducible *Sox2* null mESCs demonstrated that *Sox2* is dispensable for modulation of the Oct-Sox enhancers that regulate pluripotent-specific gene expression and instead mainly governs pluripotency in ESCs by regulating the expression of *Oct4* through other factors (Masui et al., 2007). Therefore, it is possible that *Nanog* may alleviate the requirement for *Sox2* in reprogramming by stimulating or maintaining *Oct4* expression. Indeed, *Nanog* is capable of maintaining *Oct4* expression in mESCs (Chambers et al., 2003). Thompson and coworkers also reported that *NANOG* expression enhanced the reprogramming of human fibroblasts but that it was not able to replace *SOX2* in the presence of only *OCT4* and *LIN-28* (Yu et al., 2007). This may indicate that *Klf4* is required for *Nanog* to function optimally in reprogramming and suggests that either they or the genes they modulate interact during the reprogramming process.

It is well known that ~90% of genes with promoters bound by OCT4 and SOX2 in human ESCs are also bound by NANOG (Boyer et al., 2005). Our result suggests that either *Nanog* or *Sox2* may be sufficient for collaborating with *Oct4* to modulate these genes and drive reprogramming. Although *Nanog* is not required for pluripotency, it safeguards ESCs against neuroectodermal and, to a more limited extent, mesodermal differentiation (Chambers et al., 2007; Vallier et al., 2009). Therefore, it is possible that *Nanog* functions in reprogramming by repressing differentiation signals, thereby assisting in the transition to an undifferentiated state.

Interestingly, we found that RepSox is also able to functionally replace *cMyc* in reprogramming. Together, these observations highlight the fact that small molecules may functionally replace reprogramming transcription factors at either early or late stages of the process and that they can act by different mechanisms—by inducing the expression of the gene itself, a closely related family member, or an unrelated gene that can functionally rescue the omission of the reprogramming transcription factor.

Our observation that a 1 day treatment with RepSox can relieve the requirement for transgenic *Sox2* indicates that unlike reprogramming with transgenic *Oct4*, *Klf4*, and *Sox2*, in which each transgene must be expressed for several days (Sridharan et al., 2009; Stadtfeld et al., 2008), small molecules can act as switches to induce stable gene expression changes that promote the completion of reprogramming. This could be an important concept for achieving purely chemical reprogramming given that our data show that chemicals such as RepSox can affect cellular processes differently depending on the timing of administration.

As we have shown here, there need not always be a discrete, one-to-one mapping between the functions of the reprogramming factors and their chemical replacements. Thus, it may be that reiterative screening in the presence of *Sox2* replacement molecules will be required for identifying compounds that can act in concert to replace *Oct4* and *Klf4*. However, it will be of significant interest to determine whether the novel reprogramming compounds we have identified can collaborate with those previously described (Marson et al., 2008; Shi et al., 2008a; Silva et al., 2008) to replace the remaining reprogramming genes, opening a route to purely chemical reprogramming.

EXPERIMENTAL PROCEDURES

Retroviral Infection

Retroviral infections were performed as previously described with the pMXs vector (Takahashi et al., 2007a). MEFs were infected with two to three pools of viral supernatant during a 72 hr period. The first day that viral supernatant was added was termed "day 1 post-infection." For quantification, *Oct4*::GFP⁺ colonies were counted at day 30 postinfection unless otherwise stated. All animal research was performed under the oversight of the Office of Animal Resources at Harvard University.

Small-Molecule Screens

On day 4 postinfection, infected MEFs were trypsinized and reseeded on irradiated feeders in 96-well plates at 2000 cells/well and cultured in mouse ESC media (Knockout DMEM,15% Hyclone FBS, L-glutamine, penicillin/streptomycin, nonessential amino acids, β-mercaptoethanol, and 1000 U/ml LIF). The next day, compound stock solutions diluted in DMSO and VPA (Sigma) were added at a final concentration of 1 μM and 2 mM, respectively. VPA was removed after 1 week, and the compound was reapplied every other day with each media change. Plates were scored for GFP⁺ colonies after 11 days of compound treatment.

Quantification of *Oct4*::GFP⁺ iPSCs Generated with Small-Molecule Hit Compounds, SB431542, and Tgf-β Antibodies

Retroviral infection and compound or antibody treatment was performed as in the original chemical screen. For quantification of the numbers of GFP⁺ colonies produced in different conditions, the number of colonies in each well was counted and at least two different wells were counted and averaged. Concentrations of compounds and antibodies were as follows: VPA (Sigma), 2 mM; RepSox (Calbiochem), 25 μM or 1 μM as noted; E-616451 (Calbiochem), 3 μM; EI-275 (Biomol), 3 μM; SB431542 (Sigma), 25 μM or 2 μM as noted; TgfβII-specific antibody (R&D Systems, AB-12-NA), 10 μg/ml; and pan-Tgfβ antibody (R&D Systems, AB-100-NA), 10 μg/ml. Unless otherwise noted, all chemical treatments were continuous from initial administration at day 4–5 postinfection until GFP⁺ colonies were scored at day 30 posttransduction. Fresh chemical was added at each media change.

Chemical Reprogramming of Stable Intermediate Cell Lines

Oct4::GFP-negative colonies in *Oct4*, *Klf4*, and *cMyc* or *Oct4-*, *Klf4-*, *cMyc-*, and *Sox2*-infected MEF cultures were picked and plated on irradiated feeders, and single colonies were picked after 1 week. The resulting cell lines were

passaged with trypsin and grown in mESC media on feeders until passage 4, at which time they were treated with RepSox (25 μM), AZA (500 μM), or both for 48 hr. For 2i treatment, CHIR99021 (Stemgent) was used at 3 μM and PD0325901 (Stemgent) was used at 1 μM. *Oct4*::GFP⁺ colonies were scored 12 days after the beginning of chemical treatment. Treatments were performed in mESC media containing FBS unless otherwise noted.

SUPPLEMENTAL DATA

Supplemental Data include Supplemental Experimental Procedures, 13 figures, and 2 tables and can be found with this article online at http://www.cell.com/cell-stem-cell/supplemental/S1934-5909(09)00508-6.

REFERENCES

Amabile, G., and Meissner, A. (2009). Induced pluripotent stem cells: Current progress and potential for regenerative medicine. Trends Mol. Med. *15*, 59–68.

Attisano, L., and Wrana, J.L. (2002). Signal transduction by the TGF-beta superfamily. Science *296*, 1646–1647.

Boiani, M., Kehler, J., and Scholer, H.R. (2004). Activity of the germline-specific Oct4-GFP transgene in normal and clone mouse embryos. Methods Mol. Biol. *254*, 1–34.

Boyer, L.A., Lee, T.I., Cole, M.F., Johnstone, S.E., Levine, S.S., Zucker, J.P., Guenther, M.G., Kumar, R.M., Murray, H.L., Jenner, R.G., et al. (2005). Core transcriptional regulatory circuitry in human embryonic stem cells. Cell *122*, 947–956.

Chambers, I., Colby, D., Robertson, M., Nichols, J., Lee, S., Tweedie, S., and Smith, A. (2003). Functional expression cloning of Nanog, a pluripotency sustaining factor in embryonic stem cells. Cell *113*, 643–655.

Chambers, I., Silva, J., Colby, D., Nichols, J., Nijmeijer, B., Robertson, M., Vrana, J., Jones, K., Grotewold, L., and Smith, A. (2007). Nanog safeguards pluripotency and mediates germline development. Nature *450*, 1230–1234.

Gellibert, F., Woolven, J., Fouchet, M.H., Mathews, N., Goodland, H., Love-grove, V., Laroze, A., Nguyen, V.L., Sautet, S., Wang, R., et al. (2004). Identification of 1,5-naphthyridine derivatives as a novel series of potent and selective TGF-beta type I receptor inhibitors. J. Med. Chem. *47*, 4494–4506.

Hacein-Bey-Abina, S., Von Kalle, C., Schmidt, M., McCormack, M.P., Wulf-fraat, N., Leboulch, P., Lim, A., Osborne, C.S., Pawliuk, R., Morillon, E., et al. (2003). LMO2-associated clonal T cell proliferation in two patients after gene therapy for SCID-X1. Science *302*, 415–419.

Hanke, J.H., Gardner, J.P., Dow, R.L., Changelian, P.S., Brissette, W.H., Weringer, E.J., Pollok, B.A., and Connelly, P.A. (1996). Discovery of a novel,

potent, and Src family-selective tyrosine kinase inhibitor. Study of Lck- and FynT-dependent T cell activation. J. Biol. Chem. *271*, 695–701.

Hong, H., Takahashi, K., Ichisaka, T., Aoi, T., Kanagawa, O., Nakagawa, M., Okita, K., and Yamanaka, S. (2009). Suppression of induced pluripotent stem cell generation by the p53-p21 pathway. Nature *460*, 1132–1135.

Huangfu, D., Maehr, R., Guo, W., Eijkelenboom, A., Snitow, M., Chen, A.E., and Melton, D.A. (2008a). Induction of pluripotent stem cells by defined factors is greatly improved by small-molecule compounds. Nat. Biotechnol. *26*, 795–797.

Huangfu, D., Osafune, K., Maehr, R., Guo, W., Eijkelenboom, A., Chen, S., Muhlestein, W., and Melton, D.A. (2008b). Induction of pluripotent stem cells from primary human fibroblasts with only Oct4 and Sox2. Nat. Biotechnol. *26*, 1269–1275.

Inman, G.J., Nicolas, F.J., Callahan, J.F., Harling, J.D., Gaster, L.M., Reith, A.D., Laping, N.J., and Hill, C.S. (2002). SB-431542 is a potent and specific inhibitor of transforming growth factor-beta superfamily type I activin receptor-like kinase (ALK) receptors ALK4, ALK5, and ALK7. Mol. Pharmacol. *62*, 65–74.

Kaji, K., Norrby, K., Paca, A., Mileikovsky, M., Mohseni, P., and Woltjen, K. (2009). Virus-free induction of pluripotency and subsequent excision of reprogramming factors. Nature *458*, 771–775.

Kim, D., Kim, C., Moon, J., Chung, Y., Chang, M., Han, B., Ko, S., Yang, E., Cha, K.Y., Lanza, R., and Kim, K.S. (2009). Generation of human induced pluripotent stem cells by direct delivery of reprogramming proteins. Cell Stem Cell *4*, 472–476.

Marson, A., Foreman, R., Chevalier, B., Bilodeau, S., Kahn, M., Young, R.A., and Jaenisch, R. (2008). Wnt signaling promotes reprogramming of somatic cells to pluripotency. Cell Stem Cell *3*, 132–135.

Masui, S., Nakatake, Y., Toyooka, Y., Shimosato, D., Yagi, R., Takahashi, K., Okochi, H., Okuda, A., Matoba, R., Sharov, A.A., et al. (2007). Pluripotency governed by *Sox2* via regulation of *Oct3/4* expression in mouse embryonic stem cells. Nat. Cell Biol. *9*, 11.

Meissner, A., Wernig, M., and Jaenisch, R. (2007). Direct reprogramming of genetically unmodified fibroblasts into pluripotent stem cells. Nat. Biotechnol. *25*, 1177–1181.

Mikkelsen, T.S., Hanna, J., Zhang, X., Ku, M., Wernig, M., Schorderet, P., Bernstein, B.E., Jaenisch, R., Lander, E.S., and Meissner, A. (2008). Dissecting direct reprogramming through integrative genomic analysis. Nature *454*, 49–55.

Nakagawa, M., Koyanagi, M., Tanabe, K., Takahashi, K., Ichisaka, T., Aoi, T., Okita, K., Mochiduki, Y., Takizawa, N., and Yamanaka, S. (2008). Generation of induced pluripotent stem cells without Myc from mouse and human fibro-blasts. Nat. Biotechnol. *26*, 101–106.

Okita, K., Ichisaka, T., and Yamanaka, S. (2007). Generation of germline-competent induced pluripotent stem cells. Nature *448*, 313–317.

Okita, K., Nakagawa, M., Hyenjong, H., Ichisaka, T., and Yamanaka, S. (2008). Generation of mouse induced pluripotent stem cells without viral vectors. Science *322*, 949–953.

Shi, Y., Desponts, C., Do, J.T., Hahm, H.S., Scholer, H.R., and Ding, S. (2008a). Induction of pluripotent stem cells from mouse embryonic fibroblasts by Oct4 and Klf4 with small-molecule compounds. Cell Stem Cell *3*, 568–574.

Shi, Y., Do, J.T., Desponts, C., Hahm, H.S., Scholer, H.R., and Ding, S. (2008b). A combined chemical and genetic approach for the generation of induced pluripotent stem cells. Cell Stem Cell *2*, 525–528.

Silva, J., Barrandon, O., Nichols, J., Kawaguchi, J., Theunissen, T.W., and Smith, A. (2008). Promotion of reprogramming to ground state pluripotency by signal inhibition. PLoS Biol. *6*, e253.

Silva, J., Chambers, I., Pollard, S., and Smith, A. (2006). Nanog promotes transfer of pluripotency after cell fusion. Nature *441*, 997–1001.

Silva, J., Nichols, J., Theunissen, T.W., Guo, G., van Oosten, A.L., Barrandon, O., Wray, J., Yamanaka, S., Chambers, I., and Smith, A. (2009). Nanog is the gateway to the pluripotent ground state. Cell *138*, 722–737.